2017

The pattern of perineuronal net elements in the mediodorsal thalamus

BOSTON UNIVERSITY

SARGENT COLLEGE OF HEALTH AND REHABILITATION SCIENCES

Thesis

THE PATTERN OF PERINEURONAL NET ELEMENTS IN THE MEDIODORSAL THALAMUS

by

NAYEEM MUBARAK HOSSAIN

B.S., George Mason University, 2014

Submitted in partial fulfillment of the

requirements for the degree of

Master of Science

2017

Approved by

First Reader

Helen Barbas, Ph.D.
Professor of Health Sciences
Boston University, Sargent College of Health and Rehabilitation Sciences

Professor of Anatomy and Neurobiology
Boston University, School of Medicine

Second Reader

Vasileios Zikopoulos, Ph.D.
Assistant Professor of Health Sciences

Third Reader

Miguel A. Garcia-Cabezas, MD, Ph.D.
Research Assistant Professor of Health Sciences

Acknowledgements

I thank my mentor, Dr. Helen Barbas, for her guidance and support throughout the completion of my work. I thank the members of my thesis committee, Dr. Vasileios Zikopoulos and Dr. Miguel A. Garcia-Cabezas, for their time and advice. I thank those who guided me through tissue preparation and electron microscopy, Marcia Feinberg and Tara McHugh. I thank Dr. Sabina Berretta and Dr. Harry Pantazopoulos for their prominent roles in forwarding the research of the subject matter of my thesis. I finally thank my colleagues in the lab with whom it has been a pleasure working along side, Yohan John, Iris Trutzer, Mary Kate Joyce, Jingyi Wang, and Ify Onochie.

THE PATTERN OF PERINEURONAL NET ELEMENTS IN THE MEDIODORSAL THALAMUS

NAYEEM MUBARAK HOSSAIN

ABSTRACT

Perineuronal nets (PNNs) decrease neuroplasticity, increase stability of neural systems, and are key to ending the neurodevelopmental critical period. PNNs are found throughout the brain, including the mediodorsal (MD) thalamus, a key region in cortico-thalamo-cortical communication with the prefrontal cortex (PFC). I examined the structure and location of PNN elements relative to axons in the MD thalamus from *post-mortem* human brain tissue in three normal individuals. Using electron microscopy and two-dimensional analysis, my results showed that about a third of axons have a consistent distribution of the PNN element brevican. A vital component of PNNs, the chondroitin sulfate proteoglycan (CSPG) brevican was found within the cytoplasm, within the myelin, and outside the myelin along the length of axons. Three-dimensional analyses and axon reconstructions showed that the quantity of brevican varied periodically along axons in a wave-like manner. These findings suggest a model for the arrangement of brevican in a weaving pattern through myelin, cytoplasm, and external surface of axons. This model of PNN elements has various functional implications, including influence on the growth and function of axons, ion homeostasis along the axon, and the ability of neurons to produce and transmit action potentials. These structures likely have a significant impact on the function of MD. The combined influence of PNNs and connections of the MD thalamus with the PFC may play powerful roles in various cognitive disorders, including schizophrenia.

TABLE OF CONTENTS

LIST OF FIGURES

LIST OF ABBREVIATIONS

ANOVA	Analysis of Variance
CA2	*Cornu Ammonis* Area 2
ChABC	Chondroitinase ABC
CNS	Central Nervous System
CSPG	Chondroitin Sulfate Proteoglycan
Crtl-1	Cartilage Link Protein-1
ECM	Extracellular Matrix
GABA	γ-Aminobutyric Acid
GPe	Globus Pallidus External
GPi	Globus Pallidus Internal
KO	Gene Knock Out
MD	Mediodorsal; Mediodorsal Nucleus of the Thalamus
MDl	Lateral Subdivision of Mediodorsal Thalamus
MDmc	Magnocellular Subdivision of Mediodorsal Thalamus
MDmf	Multiform Subdivision of Mediodorsal Thalamus
MDpc	Parvicellular Subdivision of Mediodorsal Thalamus
MNTB	Medial Nucleus of the Trapezoid Body
NG2	Neural/Glial Antigen 2
OIP	Object-In-Place
PFC	Prefrontal Cortex
PNN	Perineuronal Net

PTZ	Pentylenetetrazol
PV	Parvalbumin
WFA	*Wisteria Fluoribunda* Agglutinin
2D	Two-Dimensional
3D	Three-Dimensional

BACKGROUND

First observed by Camillo Golgi in 1893 and confirmed by Santiago Ramon y Cajal by 1898 (Celio, Spreafico, De Biasi, & Vitellaro-Zuccarello, 1998), perineuronal nets (PNNs) play a critical role in the formation and maintenance of neural pathways (Vitellaro-Zuccarello, De Biasi, & Spreafico, 1998). As defined structures made up of materials found in the extracellular matrix (ECM), PNNs have a key role in reducing plasticity and increasing stability of neural networks. This role is most clearly seen as the closure of the critical period during neural development, when these structures first widely appear (Berretta, 2012; Bitanihirwe & Woo, 2014; Bukalo, Schachner, & Dityatev, 2001; Carstens, Phillips, Pozzo-Miller, Weinberg, & Dudek, 2016; Carulli, Kwok, & Pizzorusso, 2016; Dityatev & Schachner, 2003; Hartig et al., 1999; Karetko & Skangiel-Kramska, 2009; Kauhausen, Thompson, & Parish, 2015; Kwok, Afshari, Garcia-Alias, & Fawcett, 2008; Lendvai et al., 2013; Nabel & Morishita, 2013; Pantazopoulos & Berretta, 2016; D. Wang & Fawcett, 2012; T. Y. Wang et al., 2016). While these unique structures are found throughout the brain, their role within the mediodorsal (MD) thalamus is of particular interest, because this thalamic nucleus plays a critical role through an intricate network of projections mainly with the prefrontal cortex (PFC).

Perineuronal Nets

Structure and Formation of Perineuronal Nets

To understand the function of PNNs within the central nervous system (CNS), one must first understand their structure. The elements of PNNs include chondroitin sulfate proteoglycans (CSPGs), hyaluronan, link proteins, and the trimeric protein tenascin-R. These components are also found in axonal coats, which may be related to PNNs. To create the relatively simple PNN structure, CSPGs must first interact with hyaluronan polymer chains at the cell surface. Link proteins, often cartilage, link protein-1 (Crtl1), then stabilize this interaction. Finally, the C-terminal domain of the CSPG core proteins binds to the trimeric glycoprotein tenascin-R to form the classic PNN structure. As countless PNNs form over time, they create a matrix which coats the neuronal surface, giving a characteristic tight net arrangement (Bitanihirwe & Woo, 2014; Karetko & Skangiel-Kramska, 2009; Lendvai et al., 2013; D. Wang & Fawcett, 2012).

When and where the formation of PNNs takes place is also of particular interest as this gives a better idea of the role these structures play in their surroundings and timing in development. With regard to the time of their formation, rodent models have shown that while many of the primary components of PNNs are seen as early as postnatal day 3, the structures themselves are not seen until postnatal day 14 (Carulli, Rhodes, & Fawcett, 2007). The formation of these structures at this later time is also associated with a sharp up-regulation of Crtl1, which appears to be the final piece necessary for the formation of functional PNNs (Carulli et al., 2010). Then there is the matter of where the elements that

compose PNNs are formed. Though many elements are equally formed by both neurons and glia (i.e., brevican) many others are formed primarily by glia (i.e., versican and Tn-R) (D. Wang & Fawcett, 2012).

It is important to note that PNNs are not found on all neurons. Numerous studies have shown that in the cortex these structures are most often found with fast-spiking inhibitory interneurons associated with the calcium binding protein parvalbumin (PV) (Balmer, 2016; Carulli et al., 2016; Yamada & Jinno, 2017). Still, while they may be found primarily on PV-interneurons, it is not an exclusive class. PNNs have also been found on excitatory pyramidal neurons within the hippocampal CA2 field (Carstens et al., 2016).

Another recent study provided evidence that specialized ECM structures are differently distributed relative to the overall composition of the ECM within the same region. By means of staining and imaging brain sections, Dauth et al. made observations on the concentration of specific ECM components, which also showed the concentration of PNNs among brain regions. Regions of focus were the amygdala, hypothalamus, thalamus, caudate-putamen, hippocampus, and isocortex (Dauth et al., 2016). The components targeted for staining were aggrecan and brevican, two CSPGs individually associated with PNNs, as well as tenascin-R, a key component of all PNNs. Aggrecan-positive PNNs were found in their highest concentration in the isocortex and their lowest in the thalamus. Brevican-positive PNNs were also found to be most concentrated in the isocortex and least concentrated in the hippocampus. These two categories of PNNs differed in their concentration across the observed regions, with brevican-positive PNNs

being less abundant overall (Dauth et al., 2016). These observations suggest that the ECM is formed and maintained for the specific functions of each brain area. To add to this, over the course of development it can be observed with increasing clarity that the distribution of PNNs is not homogeneous throughout the CNS. Using *Wisteria floribunda* agglutinin (WFA) to identify PNNs, these structures have shown a particular incremental maturation in the PFC through puberty and early adulthood (Bitanihirwe & Woo, 2014). This gradual formation is highly reflective of the functional role of PNNs in plasticity and the stabilization of neural pathways.

Effect of Perineuronal Nets on Neural Plasticity and Stabilization

With regard to the function of PNNs, the overarching conclusion in studies involving these structures is that the presence of PNNs is associated with a decrease in plasticity, but the exact means by which this decrease occurs is still highly debated (Bitanihirwe & Woo, 2014; Carulli et al., 2016; Dityatev & Schachner, 2003; Karetko & Skangiel-Kramska, 2009; Kwok et al., 2008; Pantazopoulos & Berretta, 2016; D. Wang & Fawcett, 2012). This reduction in plasticity is particularly relevant in terms of the end of the critical period of neurodevelopment. Only once PNNs are fully formed does this period come to an end.

Before going into the effect of PNNs on plasticity, it is necessary to elaborate about the nature of plasticity itself. Plasticity involves changes in neurons to enable a specific function. Plasticity of neural circuitry is based on the strengthening of synaptic

interactions through long-term potentiation as a result of increased neuronal activity as well as long-term depression through decreased neuronal activity (Bear, Connors, & Paradiso, 2007). There are distinct windows of time during which the brain is in a heightened state of plasticity, which are referred to as critical periods. The critical period is known for its high level of plasticity through experience and long-term potentiation during youth and developmental periods. While the general layout of the brain is established via genetic and intrinsic factors, an individual's interaction with the environment actively refines the intricate organization and formation of neural pathways. (Crair & Malenka, 1995; LeBlanc & Fagiolini, 2011). Use and disuse of neural pathways is also important to keep in mind as PNN formation has been correlated with an increase in experience to stabilize pathways (Carstens et al., 2016).

The classic model of plasticity and the critical period was demonstrated with eyelid suturing. Hubel and Wiesel's experiment in 1964 showed this effect by using monocular deprivation in kittens, conducted by suturing a single eye per cat very early in development, waiting an extended period of time, and then opening the eye at a later stage in development. The purpose of this suturing was to greatly reduce the amount of neural activity associated with the eye. They found that the sutured eye never gained the ability to properly form neural pathways for optimal function, suggesting that the eye was opened after the end of a critical period of activity-based neural development (Hubel & Wiesel, 1964).

The above study is quite relevant because a very similar experiment was conducted more recently, using a rodent model, with a focus on PNNs. The study

similarly used suturing to close one eye of each rodent, however a select number of rodents were also given chondroitinase ABC (ChABC) to degrade PNNs. ChABC works by degrading the key linkage glycoprotein while destabilizing the CSPG side chains that form the net-like structure of PNNs. The addition of this step had the opposite results from those reported by Hubel and Wiesel. By degrading PNNs, even the sutured eyes of rodents showed the ability to increase visual acuity as well as dendritic spine density to a healthy level identical to that of the non-sutured eye. This is particularly important because this healthy level was reached even when the eye was opened after the critical period of development (Pizzorusso et al., 2002). In this latter study, a healthy level of neural connectivity was achieved regardless of experience during the critical period.

It can be inferred from the above studies that PNNs impede the initial structuring as well as the restructuring of neural pathways. It is also important to note that while many studies use ChABC to study a neural environment without functioning PNNs, the same effects can be achieved through the use of Crtl-KO mice (Romberg et al., 2013). By using these modified mice models we can further infer that the characteristic structure of PNNs plays a prominent role in neuroplasticity.

Effect of Perineuronal Nets on Ionic Milieu

Since their degradation via ChABC results in drastic changes in function, the CSPGs of PNNs play a significant role in interaction with neurons. While there is still no definite conclusion as to how this interaction takes place, there are several hypotheses.

Among these include the idea that the neural membrane has specific receptors for the CSPGs to bind. CSPGs anchor to growth-promoting molecules and prevent access to growth promoting sites, and also aid the binding of growth-inhibitory molecules to the neuron. CSPGs are a medium by which other molecules can bind to initiate transmembrane signaling for the purpose of initiating activation of various pathways, including the PKC and Rho-Rho kinase pathway (Carulli, Laabs, Geller, & Fawcett, 2005).

To alter the function of neurons, PNNs have numerous suggested roles. One is to affect the ionic milieu surrounding the entirety of the cell. Studied primarily in GABAergic interneurons, the polyanionic character of PNNs provides a level of ion homeostasis within the microenvironment by acting as a buffering system for relevant ions. A recent study focusing primarily on potassium ions suggests that PNNs heavily influence ion concentrations. The polyanionic character of PNNs regulates the levels of potassium released by neurons during each action potential thereby preventing hyperexcitability (Bitanihirwe & Woo, 2014).

Ion homeostasis is of particular importance to fast-spiking activity, an important part of both long-term potentiation and plasticity overall. Under resting conditions, fast-spiking neurons are thought to have a large ionic current across their membranes, suggesting that these neurons are characterized by high levels of sodium ion influx and potassium ion efflux (Mendonca et al., 2016). The disproportionate amounts of sodium influx and potassium efflux could be moderated by a rapid, targeted buffering system directed toward extracellular cations. This system would result in local expansion and

contraction of the extracellular cleft, removing the need for short-distance, high magnitude, extracellular fluxes of anions (Hartig et al., 1999).

The above ionic based system might offer an explanation for the effects of PNN degradation in epilepsy. In a study with such a focus, the common method of ChABC treatment was used to degrade PNNs while pentylenetetrazol (PTZ) was used to induce seizures in rodents. PTZ is a GABA receptor antagonist used to induce convulsions using subconvulsive stimuli (Dhir, 2012). These methods produced rather interesting results as there was an increase in myoclonic seizures, but a delay of onset and decreased duration of Racine stage 4/5 seizures (Rankin-Gee et al., 2015). This study used the Racine Convulsion Scale to categorize convulsions and seizures on a five-degree scale, with the lowest referring to mild myoclonic seizures and the highest referring to severe full-body convulsions (Racine, 1972). In conclusion, the loss of PNNs resulted in a significant increase in the number of mild seizures but a significant decrease in the number and severity of seizures, suggesting a complex relationship between PNNs and seizure susceptibility (Rankin-Gee et al., 2015). Perhaps this distinct alteration might be attributed to the ChABC treatment increasing activity of specific neurons but not all. PNNs might play unique roles in regulating activity of specific neurons within a pathway.

Using a similar method of ChABC degradation of perineuronal nets, another work studied neurons with regard to the necessary conditions for depolarization. ChABC-treated neurons had numerous significant differences from control neurons in the same study (Balmer, Carels, Frisch, & Nick, 2009). One difference being that to spike, treated neurons needed more current, as the spike threshold was significantly more depolarized.

This is associated with the altered sodium ion conductance after PNN degradation. Another difference was that degradation also led to a delayed onset of spiking (Balmer et al., 2009). While this study focused on the medial nucleus of the trapezoid body (MNTB), this behavior was also seen in cortical inhibitory neurons with similar treatment (Blosa et al., 2015). Currently, there are a number of hypotheses on how PNNs might contribute to the effects on neuronal excitability. One is that they might affect the diffusion and placement of ion channels along the plasma membrane (Frischknecht et al., 2009). The highly negative charge of PNNs might significantly impact the electric field associated with gating of subunits of ion channels. Their degradation might have an impact similar to an *in vitro* extracellular introduction of a highly divalent cation solution, thereby altering membrane surface charge (Hille, 2001). This would then affect channel gating resulting in a further depolarized membrane potential and reduction in spiking (Balmer, 2016). PNNs might also function as a buffering system to stabilize the microenvironment, which can be seen by PNN degradation causing an increase in the diffusion of calcium ions in neurons (Hrabetova, Masri, Tao, Xiao, & Nicholson, 2009).

Cognitive Ramifications Associated with the Effects of Perineuronal Nets

When discussing the cellular processes within the CNS, as well as the changes in strength of neural pathways, one must also mention the cognitive ramifications of such processes. A common method of observing memory in a laboratory setting is with the use of a rodent model, through the fear response by freezing. Freezing is a natural defensive

tendency of many rodents to become still when confronted with threatening stimuli (Tovote et al., 2016). A recent study used this behavior to observe the relationship between PNNs and fear memories. The experiment began with rodents given injections of either ChABC, which degrades PNNs, or a control vehicle on day 0, followed by fear conditioning on day 1. Fear conditioning involved presenting a non-threatening stimulus paired with a threatening stimulus for the purpose of conditioning the rodent to have the freezing fear response when presented with the non-threatening stimulus alone. Remarkably, in the days following the time of injection, the rodents given ChABC showed significantly lower frequency of freezing to the initial fear stimuli in comparison to the control rodents who continued to show fear response. This effect was made more interesting by the fact that if a second fear memory was introduced to the ChABC rodents after the degradation of PNNs, it was met with rapid extinction (specific loss of memory). These observations suggest that the degradation of PNNs is associated with the erasure of fear memories. Since this type of unlearning is associated with a lack of long-term potentiation, it has been suggested that it exemplifies the role of PNNs in the stabilization of neural pathways by allowing potentiated synapses to be resistant to LTD (Bukalo et al., 2001; Gogolla, Caroni, Luthi, & Herry, 2009).

While PNNs were discovered over a century ago, there is still much we do not understand about these unique structures of the ECM. Recent years have brought a revived interest in these structures (Celio et al., 1998). My personal analyses should shed light on the interactions of PNN elements or axonal coats along individual axons as I digitally reconstructed these structures on axons of the MD thalamic nucleus.

Mediodorsal Thalamus

Structure and Connections of the Mediodorsal Thalamus

The thalamus, a word derived from the Greek meaning “inner chamber”, is a mass of grey matter composed of several nuclei that are bidirectionally connected with all areas of the cerebral cortex. With its central location within the brain, it is the major source of extracortical projections to the cortex. The MD thalamus is the major source of projections to the PFC from the thalamus (Jones, 2007), a region involved in cognition, emotion, and their integration (Fuster, 2008).

The MD thalamus is subdivided into three divisions: medial, central, and lateral. These regions are also studied with regard to their respective cell types: magnocellular in the medial region, parvicellular in the central region, and multiform in the lateral region. The differences between the cell types and locations of these subdivisions of MD have varying relationships with different areas throughout the PFC (Barbas, Henion, & Dermon, 1991; Giguere & Goldman-Rakic, 1988; Mitchell & Chakraborty, 2013). The MD thalamus is strongly connected with the PFC, and to a lesser extent, with the medial temporal lobes and subcortical regions (Barbas et al., 1991).

While the thalamus is often discussed in terms of its role in sensory perception, it is interconnected with all brain regions. Reflective of this connectivity is the unique relationship between the basal ganglia and thalamus. Though the basal ganglia receive information from around the cortex, it sends information very selectively to only some

thalamic nuclei, and specifically those that are connected with the motor, premotor, and prefrontal cortices (Barbas, García-Cabezas, & Zikopoulos, 2013). The direct and indirect pathways through the basal ganglia create a unique interconnectivity between a number of brain regions including the thalamus. The direct pathway consists of projections from around the brain to the basal ganglia, which then inhibit the globus pallidus internal (GPi). The GPi then disinhibits the thalamus, which allows for an excitatory relationship with the frontal cortex. The indirect pathway is slightly more complex than its direct counterpart. While the cortex similarly projects to the basal ganglia, the indirect pathway follows projections from the basal ganglia to the globus pallidus external (GPe), which then disinhibits the subthalamic nucleus allowing it to excite the GPi. The now excited GPi inhibits the thalamus, preventing interaction with the frontal cortex (Barbas et al., 2013). The two pathways of this circuit portray the unique relationship between the thalamus and the frontal cortex. Subcortical interactions include the fronto-striatal-thalamic circuit, with its direct and indirect pathways.

The divisions of the MD thalamic nucleus play a unique role within this circuit. The GPi primarily interacts with the MDpc and MDl, while the ventral pallidum primarily interacts with the MDmc. The basal ganglia also receive projections primarily from lateral and some midline regions of MD (Berendse & Groenewegen, 1990; Gimenez-Amaya, McFarland, de las Heras, & Haber, 1995; Groenewegen, Berendse, Wolters, & Lohman, 1990; Groenewegen, Galis-de Graaf, & Smeets, 1999; Haber & Calzavara, 2009; Haber & McFarland, 2001).

Some researchers suggest the PFC should be defined by its projections from the MD thalamus (Rose & Woolsey, 1948). Through the use of retrograde tracers to study these regions, MD was observed to make up over 80% of projection neurons from the thalamus directed to the PFC. Through histochemical and cytoarchitectonic procedures, the specificity of these projections were also observed. There is a degree of parallelism between the MD thalamus and the PFC: the medial MD thalamus is associated with the medial PFC while the lateral MD thalamus is associated with the lateral PFC (Barbas et al., 1991; Giguere & Goldman-Rakic, 1988). Giguere and Goldman-Rakic studied the specificity of projections of the MD thalamus to the PFC. This study used a method of bidirectional transport of wheat germ agglutinin conjugated to horseradish peroxidase. Almost all subdivisions of PFC were labeled in correspondence to MD regions. Overall, ventral regions of PFC (i.e. ventral surface, ventromedial cortex) are interconnected with the medial MD thalamus while dorsal regions of PFC (i.e. principal sulcus, arcuate convexity, dorsomedial areas) are interconnected with the lateral MD thalamus (Giguere & Goldman-Rakic, 1988).

The laminar organization of the PFC plays a role in the organization of these pathways, particularly regarding ipsilateral versus contralateral pathways from the MD thalamus. There are two forms of laminar organization, eulaminate in which there are six distinct layers and transitional (limbic) in which there are fewer, and less distinct layers (Dermon & Barbas, 1994). Regarding ipsilateral thalamic projections, significantly more MDmc and MDdc neurons than MDpc neurons are directed to transitional areas than eulaminate areas. Most of these ipsilateral corticothalamic projections are reciprocal.

With regard to contralateral thalamic projections, the cortical layer arrangement is critical. The contralateral thalamus projects significantly more to transitional than eulaminate areas. While ipsilateral thalamic projections go to eulaminate cortical regions, bilateral thalamic projections go to transitional cortical areas (Dermon & Barbas, 1994).

As reviewed by Jones (1998), the different types of neurochemical classes of excitatory projection neurons from the thalamus have a distinct relationship with the cortex. Calbindin neurons project to the superficial layers in a widespread manner while parvalbumin neurons project to cortical middle layers in a highly ordered manner. While thalamocortical projections carrying sensory information terminate in the middle layers of cerebral cortex in a specific manner, projections of generalized forebrain function are spread widely across the superficial layers of the cortex. This reflects the various situations which call for the recruitment of large numbers of areas or cortices and interactions across cortices resulting in their influence on one another. The diffuse projections of calbindin cells from the thalamus to cortical areas play a prominent role in corticothalamic feedback from such cortical areas, and dispersal of information throughout the cortex (Jones, 1998).

The unique relationship between MD and PFC is seen in the thalamic pathways of cortico-thalamo-cortical connections (Guillery, 1995). There are two types of communication between the PFC and the MD: driver and modulatory inputs. Driver inputs are projections from the cortex to the thalamus from layer V capable of sending signals processed in one cortical area to another cortical area (Sherman & Guillery, 2006, 2013). Modulatory inputs on the other hand, the far greater majority of connections,

significantly influence driver signals relayed to the cortex. Projections from PFC layers V and VI to higher order thalamic relay nuclei suggest that the function of these pathways is distinct from first order thalamic relays (Schwartz, Dekker, & Goldman-Rakic, 1991). Regions of the MD thalamus are reciprocally connected with both the dorsolateral and ventromedial PFC (Barbas et al., 1991; Dermon & Barbas, 1994; Giguere & Goldman-Rakic, 1988; Goldman-Rakic & Porrino, 1985; McFarland & Haber, 2002; Ray & Price, 1993; Xiao, Zikopoulos, & Barbas, 2009). These connections primarily use glutamate to communicate, showing the propagation of an excitatory signal. The fact that there are numerous regions of the PFC connected with MD suggests that there are different forms of information being sent between these regions, including information that has already been processed by the PFC (Sherman & Guillery, 2013). This interconnectivity is further strengthened by the extensive bidirectional pathways between the amygdala, MD thalamus, and pOFC which suggests a strong interaction with prefrontal areas (Timbie & Barbas, 2014, 2015).

Functions of the Mediodorsal Thalamus

The function of the MD thalamus is closely related to its interconnectivity with the PFC. Fuster and Alexander studied the functions of the MD thalamus using delayed response tasks to observe the rhythmic activity of the area (Fuster & Alexander, 1973). The delayed response task performance is a behavioral task most associated with the PFC. There was a correlation between firing changes during the behavioral task and

functional involvement and cooperation between MD and PFC. The level of overall alertness seemed to influence MD activity. This study showed that the tendency of periodic bursts of activity in MD is inversely related to the level of alertness. The disruption of rhythmic activity within MD was observed during the orientation periods of the delayed response task (Fuster & Alexander, 1973).

Seizure studies have also provided information on the nature of MD thalamus function. Petit mal epilepsy has shown involvement between MD and PFC in spontaneous rhythms similar to those of the recruiting response (Penfield, 1954). Patients who have petit real seizures have been observed to have transient episodes of depressed consciousness which are associated with activity involving both cerebral hemispheres and originating in the medial thalamus (Williams, 1953). These types of seizures and associated activity have been replicated in cats and monkeys through MD stimulation (Penfield, 1954).

The MD thalamus is most often studied through observation of cognitive and behavioral effects associated with its damage. However, the problem with this approach is that the MD is rarely damaged individually, rather it is a part of widespread damage of the surrounding region (Bradfield, Hart, & Balleine, 2013; Mitchell & Chakraborty, 2013). The interconnectivity of MD and the PFC is highlighted by disruption in executive function associated with MD damage (Carlesimo et al., 2011; Van der Werf et al., 2003; Van der Werf, Witter, Uylings, & Jolles, 2000). This form of MD damage suggests the loss of a higher order thalamic relay that supports cognitive processes of PFC. Animal models have provided a number of observations but with lack of consistency. While

studies have shown variation in results using different tasks, there is one form of task that consistently shows a significant decrease in performance (Gaffan, 2002; Mitchell, Browning, & Baxter, 2007; Wilson & Gaffan, 2008). The type of tasks affected include those that require the collaboration of information for multiple cognitive processes.

Lesion studies have been influential in the study of the MD thalamus, particularly those using non-human primates. Impairments resulting from such lesions include deficits in recognition memory, in learning of object-in-place (OIP) discriminations, object-reward associations, and performance in spatial delayed alternation tasks (Aggleton & Mishkin, 1983a, 1983b; Gaffan & Murray, 1990; Gaffan & Parker, 2000; Gaffan & Watkins, 1991; Isseroff, Rosvold, Galkin, & Goldman-Rakic, 1982; Parker, Eacott, & Gaffan, 1997; Zola-Morgan & Squire, 1985). However, there are no noticeable impairments in visual pattern discriminations or object reversal tasks, and forms of dense amnesia do not result from MD lesions themselves. In a study using tasks requiring specific strategies in response to objects, MD lesions resulted in deficits in learning new information as opposed to the retention of specific information acquired before the lesion (Mitchell & Gaffan, 2008). This observation is supported by a study in which there is a correlation between stimulus size and retention of memory, suggesting a relationship between MD and memory (Parker et al., 1997). Rodent models have further suggested these results. One study found that MD lesions at postnatal day 4 resulted in a higher frequency of anxiety associated behaviors, as well as significant abnormalities in recognition memory (Ouhaz, Ba-M'hamed, & Bennis, 2017). Another study using a patient with a MD thalamic lesion found that damage to this region significantly affects

memory (Edelstyn, Grange, Ellis, & Mayes, 2016). In a study with cats, MD lesions have been observed to ameliorate induced neurotic behaviors (Alexander & Fuster, 1973). In non-human primates, MD lesions were associated with diminishing suppression of motor conditioned responses motivated by fear without affecting associated tachycardic responses to fearful situations (Nathan & Smith, 1971). In humans, anxiety and depression have been reduced through stereotactic ablations of MD (Spiegel & Wycis, 1967).

Electrophysiological studies have provided further evidence about the interactions between the MD thalamus and the PFC (Watanabe & Funahashi, 2012). One particularly notable study focused on the relationship between these two regions in terms of dysfunction associated with schizophrenia. Dysfunction of the PFC is most often associated with schizophrenia based on the complex cognitive abnormalities associated with the pathology. A pharmacogenetic approach was used to disrupt MD-PFC synchrony in an attempt to observe altered activity during performance of the t-maze task. During the choice and reward phase of a t-maze task, mice showed significantly decreased MD activity which correlated with cognitive deficits (Parnaudeau et al., 2013).

Extensive projections between the PFC and the MD thalamus suggest that the MD thalamic nucleus might be involved in the various dysfunctions of schizophrenia (Friston & Frith, 1995). Over the years there have been numerous studies investigating this possibility, but have produced mixed results. Contradictory findings may be related to the fact that many of these studies were low resolution imaging studies examining changes in the size of MD in schizophrenia, with some finding a significant decrease in size of the

structure while others finding no change in schizophrenic individuals (Alelu-Paz & Gimenez-Amaya, 2008).

In this study, I took a different approach and investigated the ECM of this region, specifically PNN elements of axons and axonal coats in the MD thalamus at very high resolution.

Perineuronal Nets within the Mediodorsal Thalamus

The role of PNNs within the MD thalamus has been studied using a number of different methods. One study observed that during Racine stage 4/5 seizures there was a significant increase in interaction between the MD thalamus and hippocampus (Zhang et al., 2016). Another study found that low-frequency stimulation of the MD thalamus induces fluctuations of synaptic transmission in the PFC (Herry, Vouimba, & Garcia, 1999).

There have been numerous studies suggesting that dysfunction of PNNs within the MD thalamus may be a major contributor to schizophrenia pathology. This abnormality may stem from dysfunction of pathways from the MD thalamus to regions of the frontal cortex (Byne et al., 2002; Janssen et al., 2012; Kim et al., 2008; Kito, Jung, Kobayashi, & Koga, 2009; Martins-de-Souza et al., 2010; Pakkenberg, 1990; Popken, Bunney, Potkin, & Jones, 2000). There is evidence suggesting that an abnormality in CSPG based ECM structures is a major contributing factor to this dysfunction

(Kucharova & Stallcup, 2010; Lau et al., 2012; Pantazopoulos, Woo, Lim, Lange, & Berretta, 2010; Pendleton et al., 2013; Siebert & Osterhout, 2011).

Schizophrenia is accompanied by a number of cognitive abnormalities which severely affect several mental processes. These abnormalities include significant problems with attention, perception, and cognition, all of which can be physiologically traced to the thalamus (Byne et al., 2002). For this reason, it is imperative to investigate thalamic pathways and the extracellular factors that affect their function. Schizophrenia pathology is also closely associated with abnormalities involving PNNs (Berretta, 2012; Bitanihirwe & Woo, 2014).

PNNs have a distinct distribution in each region of the brain (Dauth et al., 2016). With this in mind we can explore the relationship between these structures and the MD thalamus. Using immunohistochemistry and mass spectrometry, Dauth et al. 2016 suggest that while there is still a significant presence of PNN associated proteins (aggrecan, brevican, tenascin-R) within the MD thalamus, this presence is significantly less than that of other observed brain regions. Since PNN production is activity dependent, this may reflect the degree of plasticity of the MD thalamus relative to other regions of the brain.

Through the MD thalamus we can also better understand the nature of PNNs. These structures were first observed within the ECM, described to be made up of components from the ECM, and suggested to be present outside the cell membrane as well as the myelin sheath (Vitellaro-Zuccarello et al., 1998). Along axons these ECM

components form axonal coats, but we know virtually nothing about them. However, these structures could be present in other parts of the axonal domain. The relative location of these structures may affect the nature of their function and influence on associated neurons. By exploring the placement with respect to the myelin and cell membrane in search of these structures we may better understand PNNs.

In summary, perineuronal nets and their associated axonal coats influence neuroplasticity throughout the brain and may play a role in thalamocortical communication. In this context, the overarching goal of my study was to examine components of PNNs and axonal coats in terms of their location along the length of axons within the MD thalamus in the brains of the normal human brain. With these observations I was able to extrapolate information on the location and by consequence suggest possible functions of these ECM structures.

METHODS

Experimental Design

The objective was to investigate the structure and location of axonal coats in *post-mortem* brain sections from normal human individuals (n = 3) through the MD thalamus. I used a combination of immunohistochemistry and electron microscopy to study variations in location and structure of axonal coats as well as variations in axon diameter. I used several forms of two-dimensional analysis as well as three-dimensional axonal reconstruction to study axonal coats and their associated axons.

Immunohistochemistry and Electron Microscopy

The processing and labeling of tissue for serial electron microscopy poses various challenges for *post-mortem* human brain tissue. These include limited control over *post-mortem* interval, tissue extraction protocols, and degradation of tissue. Several protocols have been used to address these issues to maximize labeling specificity and tissue quality (Zikopoulos & Barbas, 2010). These protocols helped reduce non-specific background staining, enhance penetration of reagents, minimize degradation of fine structures and decrease potential tissue damage. They also increased tissue quality allowing for 3D quantitative reconstruction of axons (Zikopoulos & Barbas, 2010).

Brain tissue fixed in formaldehyde of normal individuals (n=3) was obtained from the McLean Hospital in Belmont, MA. Thin sections of tissue (50 μm) through the

thalamus were cut and processed first with pre-embedding immunohistochemistry using antibodies against the protein brevican or the neural/glial antigen 2 (NG2). For each case, 1 thin section was processed with immunohistochemistry with a brevican marker and 1 thin section with an NG2 marker. Parts of these sections containing MDl were then processed for electron microscopy and embedded in a hard resin; 1 small block was dissected from each thin section embedded in resin and cut with an ultramicrotome (Ultracut; Leica) in series of ultrathin sections (50 nm, ~100 per block) with a diamond knife (Diatome). Single slot grids were then used to collect these ultrathin sections that were viewed with a transmission electron microscope (100CX; Jeol) (Zikopoulos & Barbas, 2006, 2007, 2010). Photomicrographs were taken of every other electron micrograph field at 6,600X with a digital camera (Gatan) attached to the electron microscope. Randomness for axon sampling was introduced by numbering each image nonconsecutively. The darkly stained electron dense myelin sheath was an identifying feature of myelinated axons at the electron microscope (Peters, Palay, & Webster, 1991; Zikopoulos & Barbas, 2010).

Photomicrograph Analysis and Axon Reconstruction

Two-Dimensional Analysis of Randomly Selected Photomicrographs

To study the incidence of markers' location I counted and categorized 24,148 axons from 61 photomicrographs (case 1: brevican = 11 photomicrographs-4,046 axons; NG2 = 10 photomicrographs-4,669 axons; case 2: brevican = 10 photomicrographs-4,260

axons; NG2 = 10 photomicrographs-3,957 axons; case 3: brevican = 10 photomicrographs-4,423 axons; NG2 = 10 photomicrographs-2,793 axons). Randomness was achieved by numbering photomicrograph fields at random. I viewed photomicrographs and traced each axon with a different color and labeled structures using Reconstruct software; I used the same program to study axon diameter in 24,148 axons (Fiala, 2005). I used three categories to analyze the location of marker interaction: *within cytoplasm or myelin*, *outside of myelin*, and *no interaction*. The tracings used to categorize these axons also provided the data necessary to calculate axon diameters. Data were exported to Excel for quantitative analysis.

Each axon tracing takes the form of an ellipse. The software used (Reconstruct) provided the area of each of these tracings. Using this area I calculated the axon diameter, which was the minor axis of each ellipse, using the following equation.

$$4 \text{ area} / (\text{major axis})\pi = \text{minor axis}$$

I then repeated this process for all axon diameter measurements. The minor axis of the traced ellipse of each axon was used to accurately measure the diameter of each axon while avoiding any influence of the angle at which the tissue was cut.

Three-Dimensional Analysis of Short Series

To study the incidence of brevican marker's location relative to the axon I studied 231 axons in 48 photomicrographs taken of short series of ultrathin sections (case 2: 1

block). Photomicrographs were taken from eight spans of six consecutive sections from numerous equidistant locations within each series of photomicrographs, i.e. four sampled series of photomicrographs consisted of sections 1–6, 51–56, 101–106, and 151–156. The goal was to study these 300 nanometer lengths of axons for a more in-depth version of the previous analysis. This was an appropriate length to analyze because if there is a consistent variance in marker location across this brief length, such variance is likely found along the entire axon. I analyzed the axons of these sections by recording the incidence of marker interaction in three categories: *within cytoplasm*, *within myelin*, and *outside of myelin*. Counted axons received only one category.

Three-Dimensional Axonal Reconstruction in Long Series: Marker Location and Axon Length

To study the incidence of brevican marker's location relative to the axon in greater detail I reconstructed a field of 35 axons from a series of consecutive photomicrographs (case 2: 1 block, 107 ultrathin consecutive sections, brevican marker). These reconstructions were created with a degree of transparency to observe whether the marker is located inside or outside the axon. The color of each axon's reconstruction was dependent on their interaction with the marker. To study the length of these axons, the same reconstructions were used. I analyzed the axons of these sections by recording the incidence of marker interaction in three categories: within cytoplasm, within myelin, and

outside of myelin. Counted axons received only one category. These full reconstructions were made using semi-transparency to study the marker both within and outside the axon.

Three-Dimensional Axonal Reconstruction in Long Series: Marker Depth and Position Relative to Myelin Sheath

To study the quantity of the brevican marker located in each region of the axon and myelin sheath in greater detail I reconstructed the axon, myelin sheath, and associated marker of 4 axons of a wide range of length (case 1: 1 block, 86 ultrathin consecutive sections) using Reconstruct and then within 3D Studio Max. The marker was reconstructed relative to three regions of the axon: *within cytoplasm,* for presence beneath the myelin sheath, *within deep myelin,* describing presence within the deep 50% of the myelin sheath, and *within superficial myelin,* describing presence in the superficial 50% or outside of the myelin sheath. I analyzed the axons of these sections by recording the incidence of marker interaction in three categories: *within cytoplasm*, *within myelin*, and *outside of myelin*. Each analyzed axon received only one category.

This analysis included axons with lengths of 4.47 µm, 4.47 µm, 11.62 µm, and 26.24 µm. To analyze quantities of marker at different depths of each axon, I calculated the surface diameter of each category of marker individually from each photomicrograph of the series. I then calculated the categorical surface diameters as percentages of the total marker surface diameter within each photomicrograph for each axon. The axon diameters

were also determined for axons 2–4. This analysis was repeated across all sections within the series for each axon.

Statistical Analysis

For the two-dimensional analysis of randomly selected sections I used Welch two sample t-tests to make comparisons between marker interaction categories. This was done for the number of axons as well as axon diameter within each category across cases. For two-dimensional analysis of sampled series I used an Analysis of Variance (ANOVA) to compare among categories of marker interaction. For three-dimensional axonal reconstructions I used Welch two sample t-tests to compare axon lengths between axons of different marker interaction categories. In all statistical analyses, the value of $P<0.05$ was used to determine significance.

RESULTS

This study used four sets of analyses. With each successive form of analysis I used fewer axons, while each axon was observed with significantly greater detail. My first analysis was based on a two-dimensional study of 24,148 axons. These axons were from randomly selected photomicrographs to investigate the interactions of markers for brevican and NG2 occurring within an axon's cytoplasm, myelin, or outside of the axon. In a second analysis, I used 231 axons for a more detailed assessment in 3D, to study the relative location of a marker over a 300 nm length of axon. These studies were designed to determine if the location of the brevican marker varies along the length of an axon. In a third analysis, I used 35 axons for a more detailed assessment in 3D. To study these I used full series of reconstructed axons to examine whether the brevican marker interaction occurred in a weaving pattern along an axon's length. Finally, my fourth analysis consisted of a 3D study of 4 axons at the greatest degree of detail. I used these axons to determine if there is periodically varying amount of brevican marker found at different depths of reconstructed axons.

Two-Dimensional Analysis of Randomly Selected Photomicrographs

Marker Location

I counted and categorized 24,148 axons based on their individual interactions with the markers for brevican or NG2. Using these axons I studied the incidence of marker interaction occurring within the cytoplasm, myelin, or outside the myelin. I used three

categories of interaction based on marker location: *within cytoplasm or myelin*, *outside of myelin*, and *no interaction*. Figure 1 shows a sample of this categorization in one of the photomicrographs, each of which had an average of 396 axons.

In photomicrographs associated with the brevican marker, 17.14% of axons had the marker within the myelin or cytoplasm, 9.54% of axons had the marker outside of the myelin sheath, and 72.92% of axons had no interaction with the marker. In photomicrographs associated with the NG2 marker: 15.02% of axons had the marker within the myelin or cytoplasm, 6.45% of axons had the marker outside of the myelin sheath, and 78.53% of axons had no interaction with the marker.

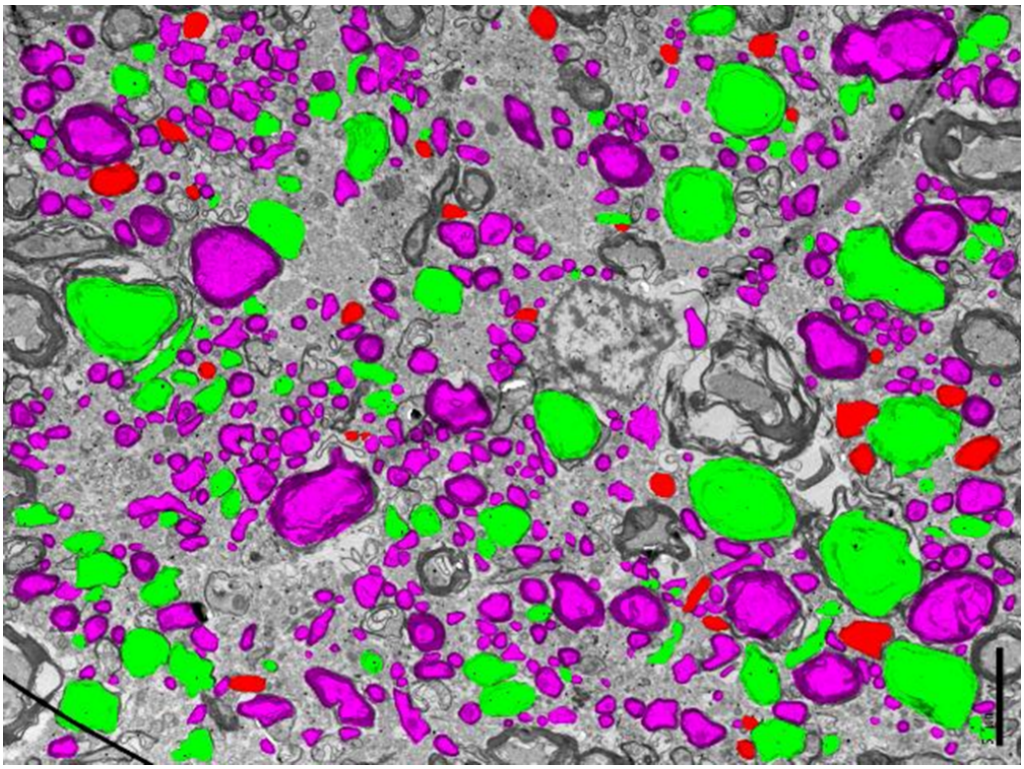

FIGURE 1 Example of axon tracing and categorization using a photomicrograph. This form of analysis used three categories of marker interaction: *within cytoplasm or myelin* (green), *outside of myelin* (red), *no interaction* (magenta). In addition to counting, tracing also measured diameter of axons. Counted axons received only one category each.

To statistically test whether the marker interactions occur more often (within cytoplasm or myelin, or outside the myelin) these percentages were then analyzed using Welch two sample t-tests to compare between interaction categories. Figure 2 summarizes these statistical analyses, which provided three significant differences. First, in photomicrographs associated with the brevican marker, the average percentage of axons with marker within the cytoplasm or myelin was significantly different from the average percentage of axons with marker outside of myelin ($P<0.001$). Second, in photomicrographs associated with the NG2 marker, the average percentage of axons with marker within the cytoplasm or myelin was significantly different from the average percentage of axons with marker outside of myelin ($P<0.001$). Third, of all photomicrographs, the average percentage of axons with marker within the cytoplasm or myelin was significantly different from the average percentage of axons with marker outside of myelin ($P<0.001$).

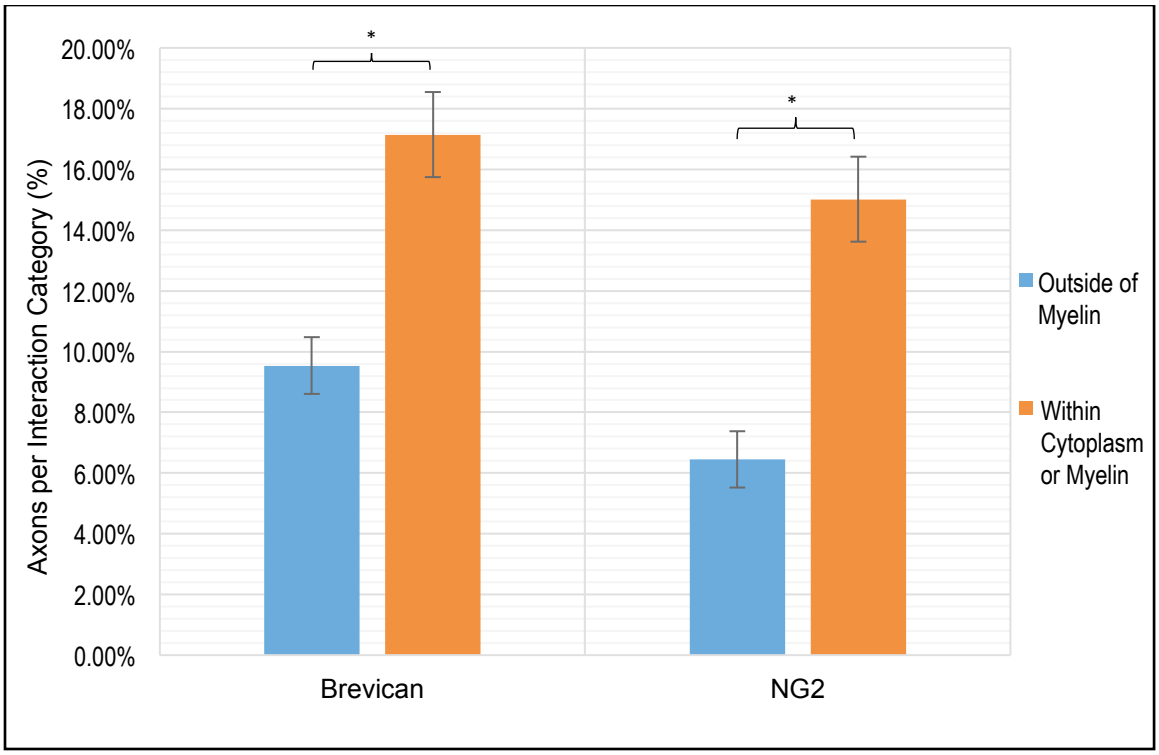

FIGURE 2 Percentage of axons in each interaction category. The number of axons of each category were calculated as a percentage of all axons. Welch two sample t-tests showed three significant differences: between the average percentage of axons with the brevican marker within cytoplasm or myelin and that of axons with the brevican marker outside of myelin ($P<0.001$), between the average percentage of axons with the NG2 marker within cytoplasm or myelin and that of axons with the NG2 marker outside of myelin ($P<0.001$), and between the average percentage of axons with either marker within cytoplasm or myelin and that of axons with either marker outside of myelin ($P<0.001$). Counted axons received only one category. The no-interaction category is not shown in this graph for greater clarity. Vertical bars represent standard error.

Axon Diameter

In addition to studying marker location, I also used the 24,148 axons to study axon diameters with regard to marker interactions. Axons with the brevican marker within the myelin or cytoplasm had an average diameter of 0.99 µm, axons with the marker outside the myelin had an average diameter of 0.76 µm, and axons with no interaction with the marker had an average diameter of 0.62 µm. With regard to the NG2 marker, axons with the marker within the myelin or cytoplasm had an average diameter

of 0.70 μm, axons with the marker outside the myelin sheath had an average diameter of 0.60 μm, and axons with no interaction with the marker had an average diameter of 0.53 μm. Figure 3 shows the average axon diameter of each category within each case.

	Average Axon Diameter (μm)		
Case	Marker Within Cytoplasm or Myelin	Marker Outside of Myelin	No Interaction
1	0.77	0.65	0.64
2	0.76	0.63	0.48
3	1.00	0.77	0.61

FIGURE 3 Average diameter of axons associated with the NG2 marker. Axons with marker were thicker than those without marker.

To determine if there is a correlation between diameter and marker interaction, I used Welch two sample t-tests to compare categories. As seen in Figure 4, these tests showed three significant differences, in diameters between the axons of different categories. Of axons with the brevican marker, the average diameter of axons with marker within the cytoplasm or myelin was significantly different from the average diameter of axons with marker outside of myelin ($P = 0.006$). Of axons with the NG2 marker, the average diameter of axons with marker within the cytoplasm or myelin was significantly different from the average diameter of axons with marker outside of myelin ($P = 0.016$). Of all axons with marker interaction, the average diameter of axons with marker within the cytoplasm or myelin was significantly different from the average diameter of axons with marker outside of myelin ($P = 0.001$).

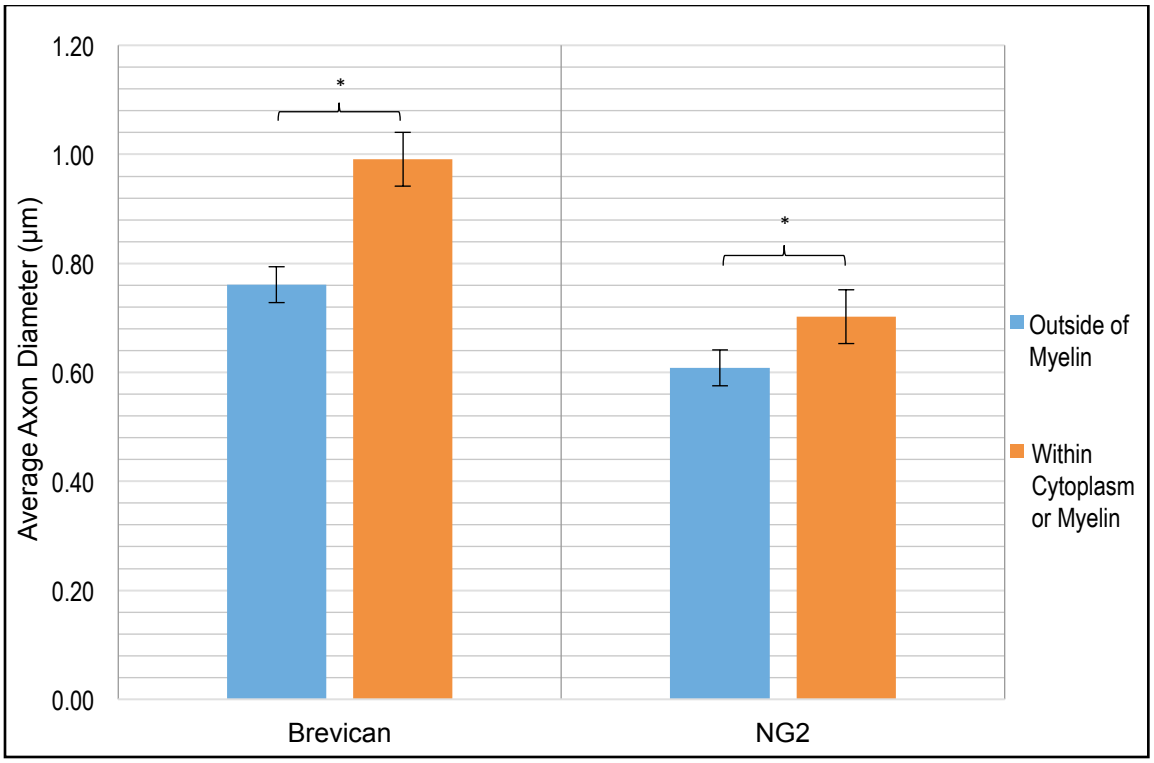

FIGURE 4 Mean axon diameter of each marker interaction category. Welch two sample t-tests showed three significant differences: between the mean diameter of axons with brevican marker within cytoplasm or myelin and that of axons with brevican marker outside of myelin (P = 0.006); the mean diameter of axons with NG2 marker within cytoplasm or myelin and that of axons with NG2 marker outside of myelin (P = 0.016); and the mean diameter of all axons with marker within cytoplasm or myelin and that of all axons with marker outside of myelin (P = 0.001). Vertical bars represent standard error.

To summarize, there were two major points in the aforementioned analyses. First, the average percentage of axons with marker within the cytoplasm or myelin was significantly different from axons with marker outside of myelin. Second, the average diameter of axons with marker within the cytoplasm or myelin was significantly different from that of axons with marker outside of myelin.

Three-Dimensional Analysis of Short Series

The next analysis included study of 231 axons from numerous short series of electron photomicrographs. I examined a total of 1,745 incidences of categorical placement of the marker within this analysis. Every axon analyzed fell into several categories along the length of each sampled region. I then calculated the relative percent of each category of interaction from the total number of incidences within each sampled series.

Statistical analysis consisted of an ANOVA comparing these percentages relative to category. There was no significant difference ($P = 0.099$) between the number of incidences between interaction categories. Figure 5 shows that incidences of marker placement are of similar frequencies, approximately one-third of the total number of incidences each, across all three categories.

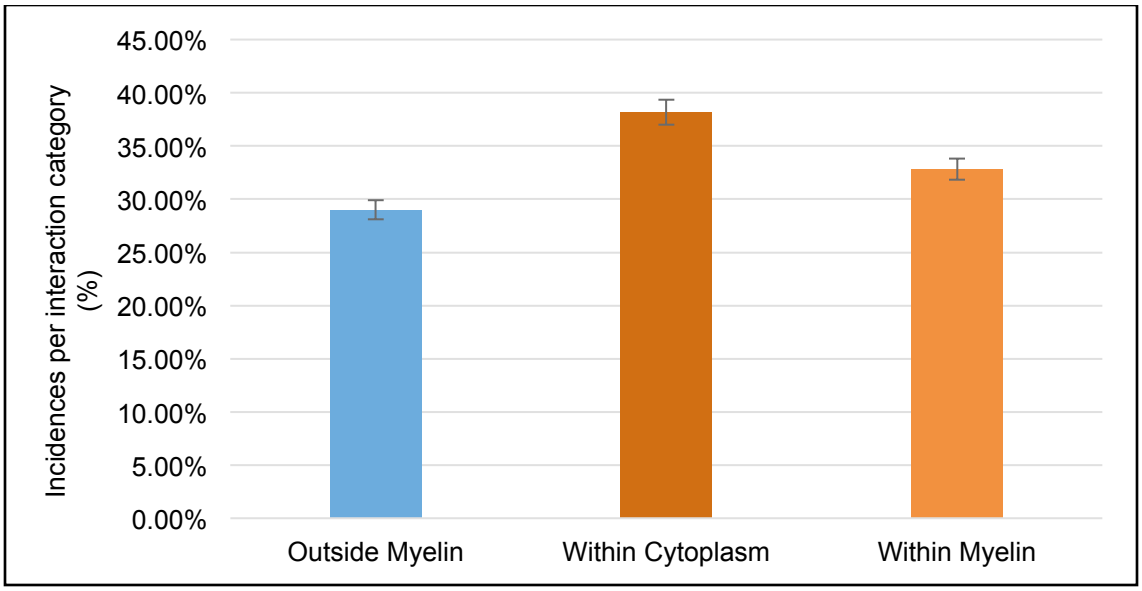

FIGURE 5 Proportion of incidences per category of marker interaction in axons. Incidences per interaction categories were compared using ANOVA. There was no significant difference (P = 0.099) between incidence rates of categories of marker interaction. Vertical bars represent standard error.

To summarize, the incidences of interaction do not have significantly different frequencies across regions of axons. A noteworthy difference between the first analysis and the second is the number of categories, as reflected in Figures 2 and 5. In my first analysis, as seen in Figure 2, I studied the marker within the cytoplasm and the marker within the myelin as one category, while in my second analysis, as seen in Figure 5, I studied these in two separate categories. The separation of these two categories provided a clearer representation of the concentrations of marker in different regions of the axon.

Three-Dimensional Axonal Reconstruction in Long Series: Marker Location and Axon Length

Marker Location

For the next analysis I reconstructed 35 axons to study whether a marker is outside of the myelin, within the myelin, within the cytoplasm, or weaving through the length of the axon. I created these reconstructions by tracing axons and their brevican marker.

As seen in Figure 6, while the marker (green) is seen exclusively along the outside of some axons (blue) there is a greater number of axons where the marker is seen both inside and outside the axon (magenta) in a weaving pattern along the length of the axon. Figure 6 also shows isolated close ups of both of these interactions.

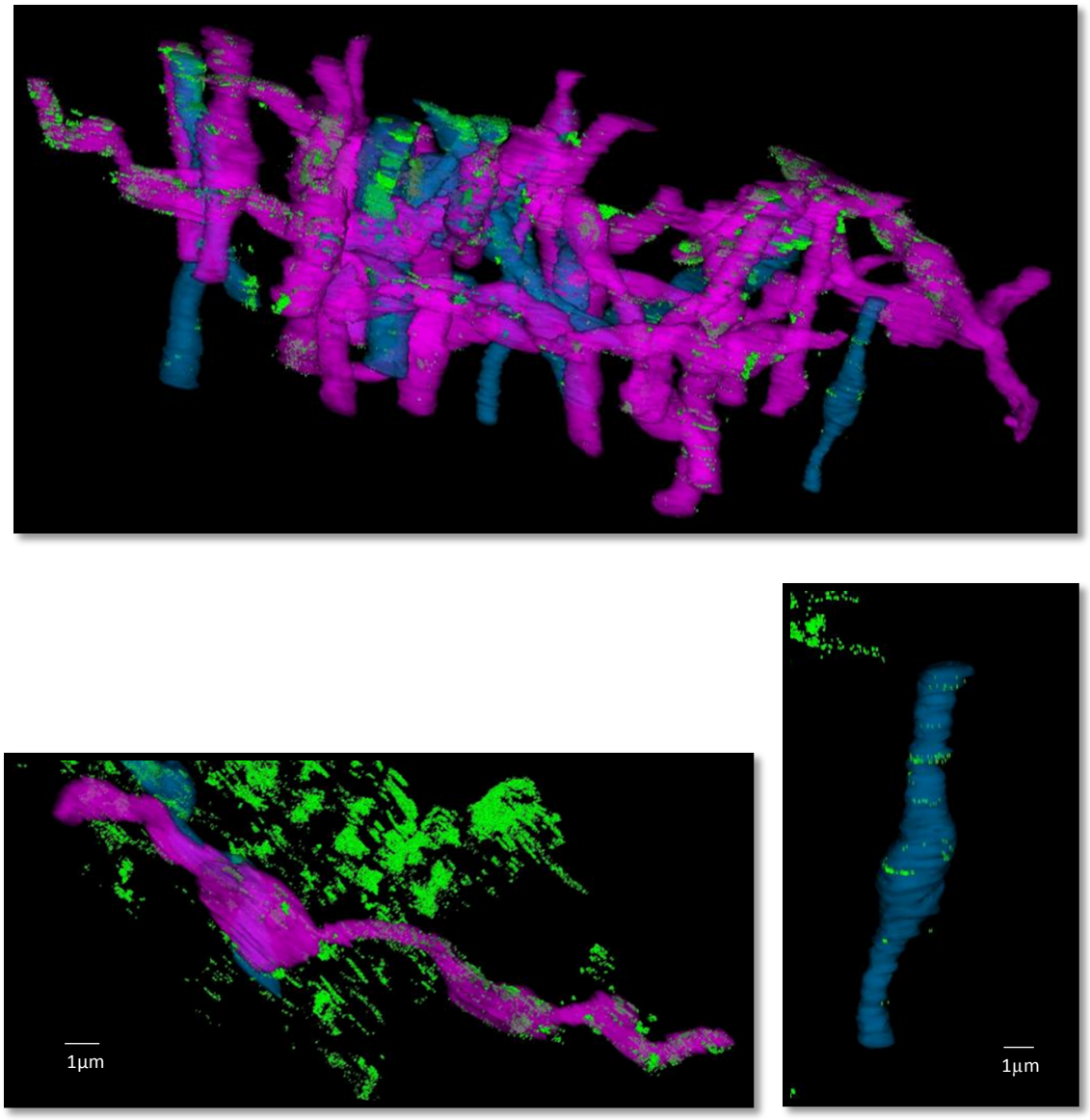

FIGURE 6 Marker location in axon reconstructions. Reconstructions were created with a degree of transparency to allow the marker to be seen both within and outside the axon. (Top) Of the thirty-five reconstructed axons, twenty-two had the marker weaving through the axon (magenta). The remaining thirteen had the marker only outside of the axon (blue). (Bottom, left) An isolated axon with the marker weaving through its length. (Bottom, right) An isolated axon with the marker only outside of the axon.

Axon Length

In addition to this qualitative analysis, I used the length of these axons for statistical analysis. Since all axons were categorized based on brevican marker interaction, I used a Welch two sample t-test to investigate if the lengths of axons differed relative to category or not. As seen in Figure 7, the length of axons with marker weaving was significantly different (P = 0.004) from the length of axons with the marker only outside of the axon.

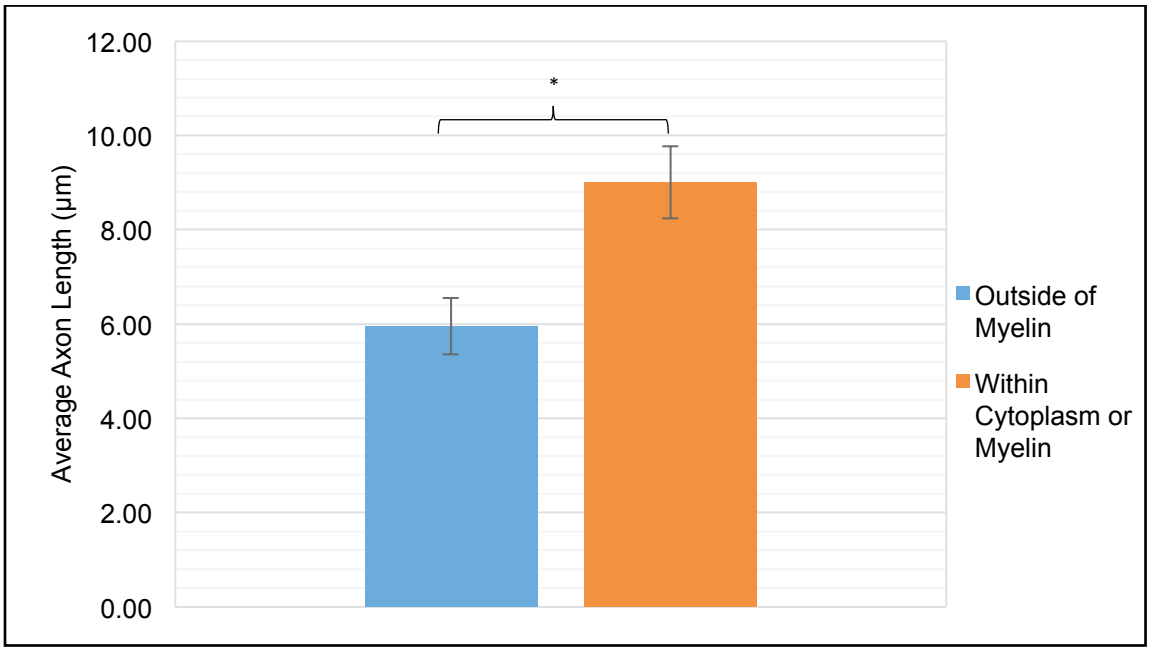

FIGURE 7 Average axon length relative to interaction category. The two categories of axons were compared relative to their lengths by means of a Welch two sample t-test. The lengths of axons with marker interaction within the cytoplasm or myelin was significantly different (P = 0.004) than those with marker interaction outside of myelin.Vertical bars represent standard error.

To summarize, while 22 of 35 axons had the marker weaving through them, these axons had a significantly different length than those without marker weaving through the axon.

Three-Dimensional Axonal Reconstruction in Long Series: Marker Depth and Position Relative to Myelin Sheath

While I used the previous analyses to study the *incidence* of each marker, in the following analysis I studied the *quantities* of marker. This parameter provided information on the location of varying quantities of marker regarding axon depth.

I traced each axon both beneath its myelin sheath as well as above it. This tracing technique created a clearer image of the axon as well as the myelin sheath. It also allowed study of the myelin along the length of each axon. In addition to this detailed tracing of the axon, I traced the brevican marker and organized it into three categories relative to position within the axon: *within cytoplasm,* for presence beneath the myelin sheath, *within deep myelin* for marker within the deepest 50% of the myelin sheath, and *within superficial myelin* referring to the superficial 50% or along the outside of the myelin sheath. I then used the tracing to reconstruct axons as seen in Figures 8–10.

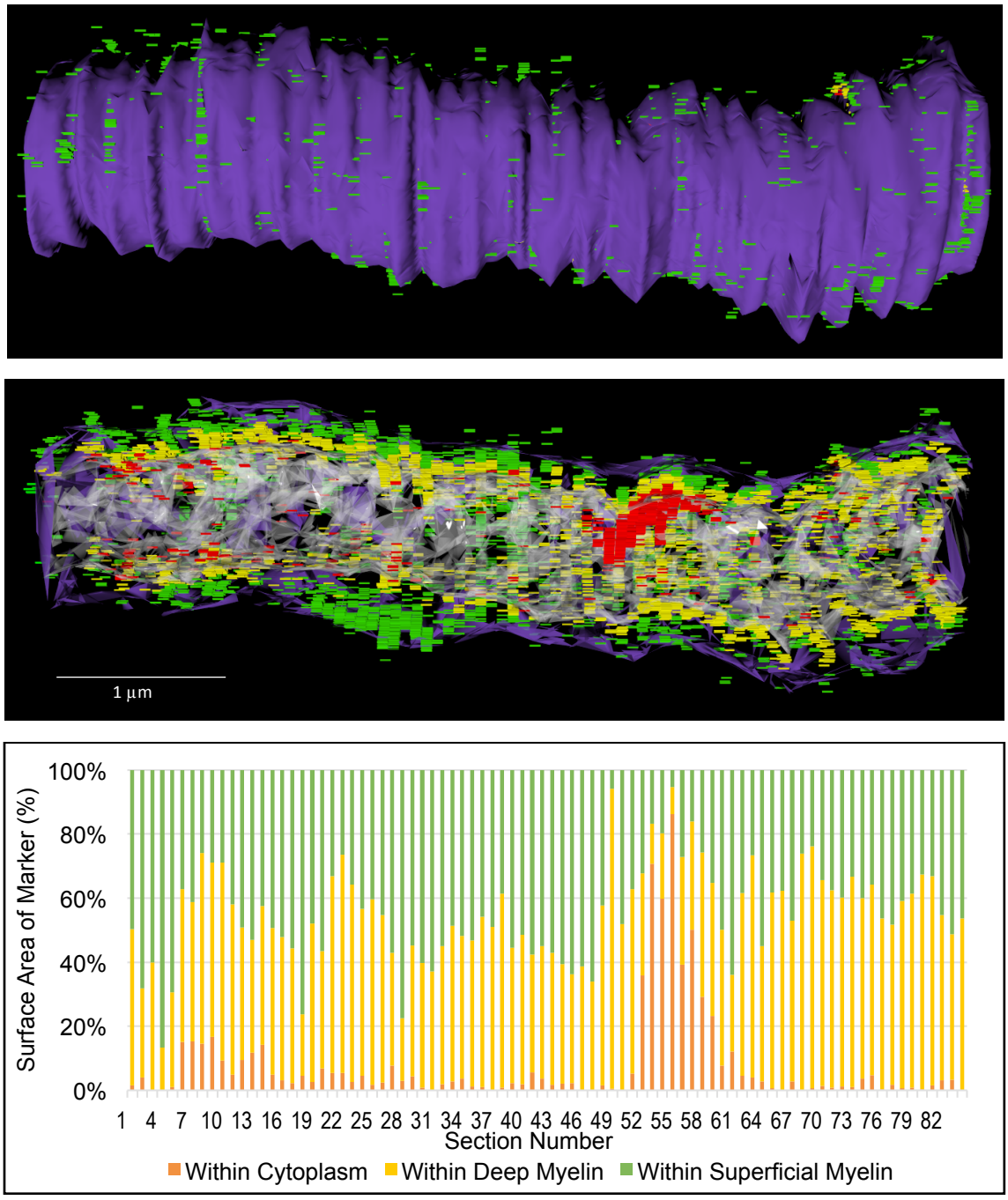

FIGURE 8 Reconstruction and analysis of Axon 1 (Sections = 1–86; length = 4.47 µm). (Top) Axon reconstruction with marker on the outside of the axon. (Middle) Axonal reconstruction with marker inside the axon where the marker can be seen in various regions beneath and within the myelin sheath. Key: Purple, myelin; white, cytoplasm; red, marker within cytoplasm; yellow, marker within deep myelin; green, marker within superficial myelin. (Bottom) Quantitative analysis of the marker category percentage relative to region across all sections. Calibration bar in Middle applies to Top and Middle.

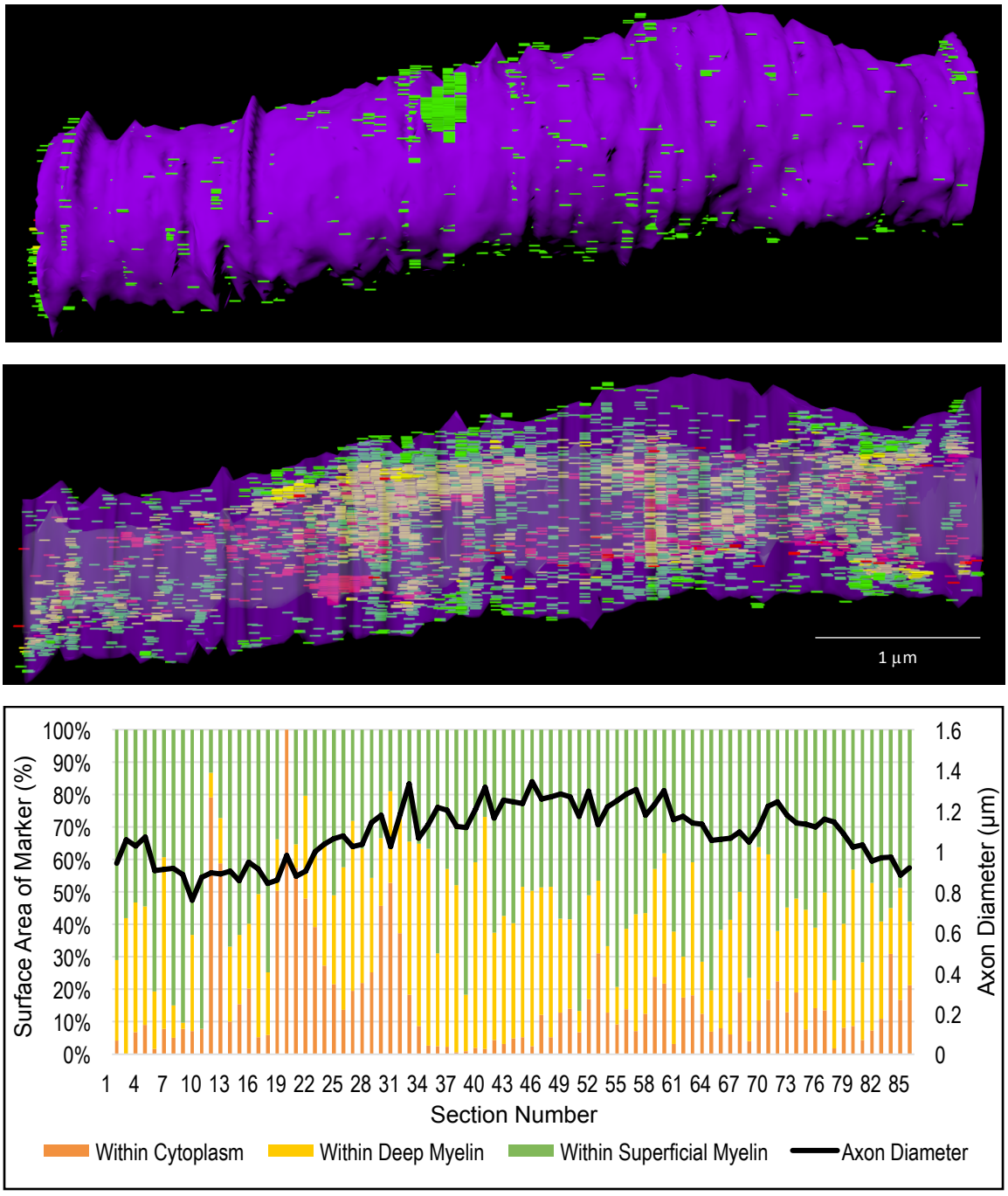

FIGURE 9 Reconstruction and analysis of Axon 2 (Sections = 1–86; length = 4.47 µm). (Top) Axon reconstruction with marker on the outside of the axon. (Middle) Axonal reconstruction with marker inside the axon where the marker can be seen in various regions beneath and within the myelin sheath. Key: Purple, myelin; white, cytoplasm; red, marker within cytoplasm; yellow, marker within deep myelin; green, marker within superficial myelin, black line, diameter. (Bottom) Quantitative analysis of the marker category percentage relative to region across all sections. Calibration bar in Middle applies to Top and Middle.

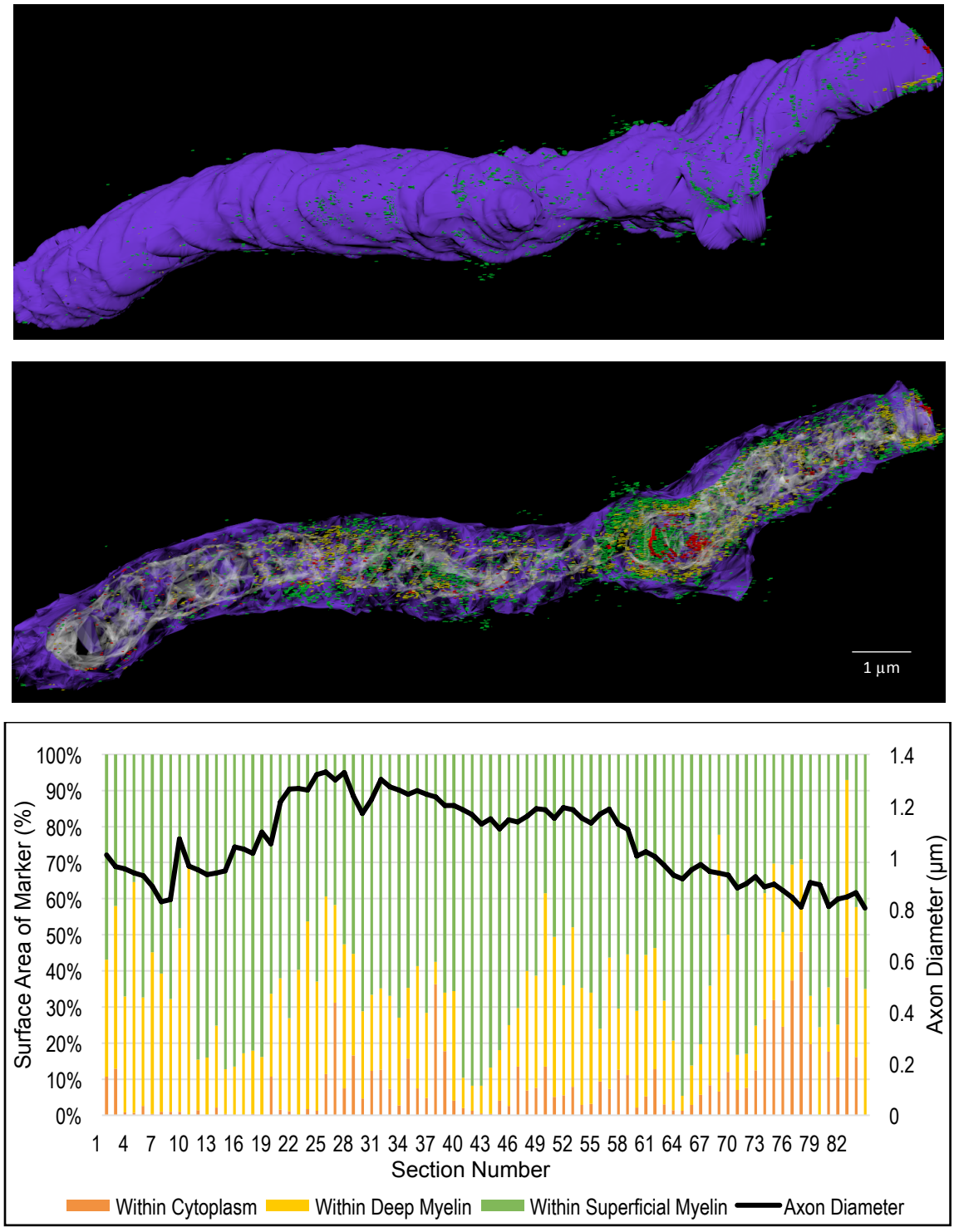

FIGURE 10 Reconstruction and analysis of Axon 3 (Sections = 1–86; length = 11.62 µm). See caption of Figure 9 for explanation.

As seen in Figures 8–10, by comparing across sections, the quantity of marker found at different depths varied along the length of the axon in a wave-like manner. The marker was found to be *within the cytoplasm*, *within deep myelin*, and *within superficial myelin* in systematically varying quantities along the length of each axon. This variation in quantity reflected alternations of high and low concentrations of marker in each region of the axon. The wave-like formation of this variance reflects the weaving pattern seen in the previous analyses. The analyses associated with the axon seen in Figures 11–12, the longest axon, was reconstructed from longitudinal sections. This axon was in a particularly longitudinal orientation as opposed to the orientation of the axons in Figures 8–10. This is likely why Figure 11 shows the last axon with numerous slices instead of one to best portray the marker along the length of this much longer axon. The quantitative analysis of this axon is also slightly different from those of Figures 8–10. As seen in Figure 11, the length of this axon is separated into 24 bins, each of which is one micron of axon length. These bins were then analyzed using a similar method as previous axons using bins in place of sections. In addition to this analysis, the axon diameter was analyzed relative to each bin as well.

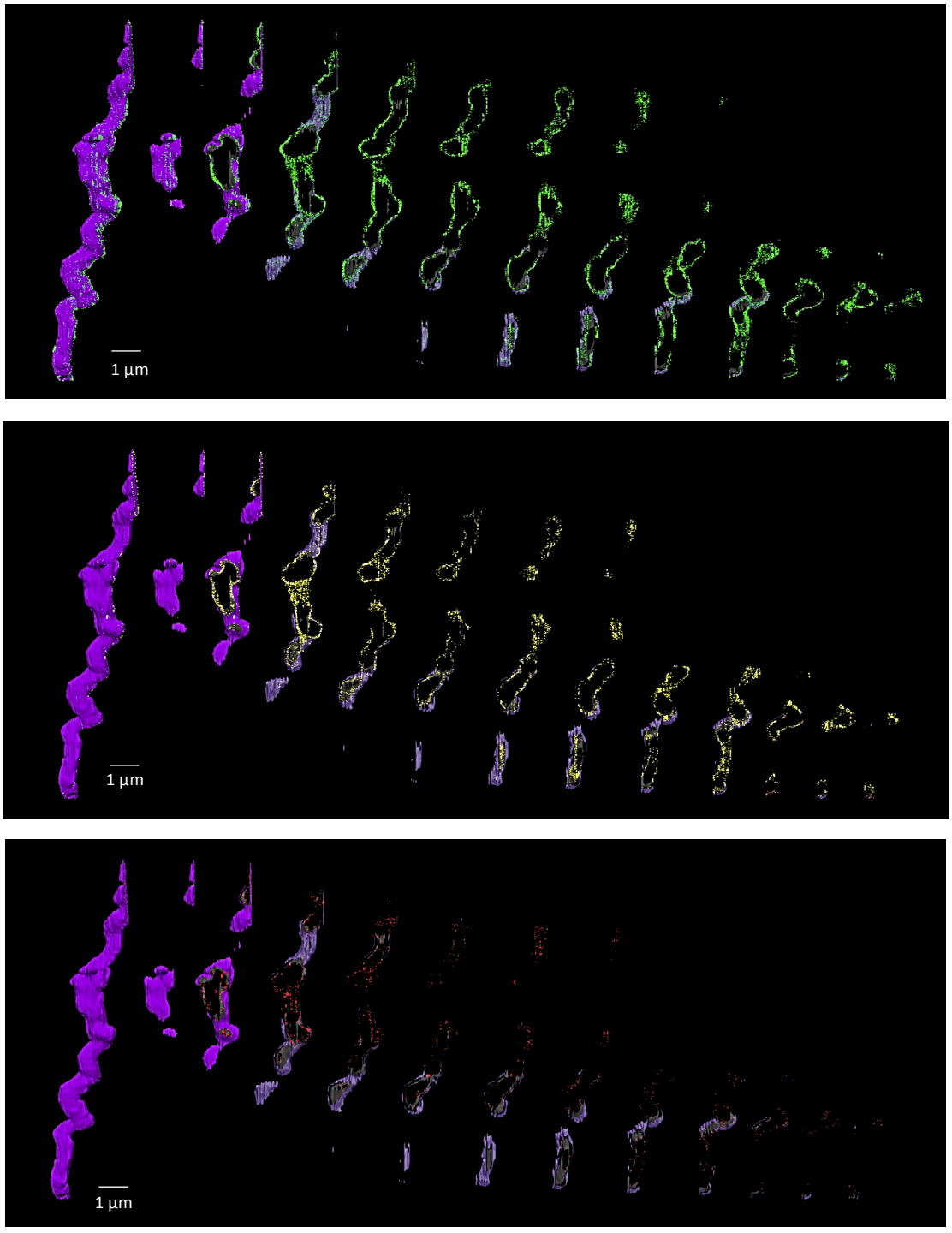

FIGURE 11 Reconstruction of Axon 4 (26.24 µm). The axon reconstruction is shown first as a whole on the left then in 12 consecutive slices. (Top) Reconstruction shown with marker within superficial myelin. (Middle) Reconstruction shown with marker within deep myelin. (Bottom) Reconstruction shown with marker within cytoplasm. (Key) Purple, myelin; white, cytoplasm; red, deep marker; yellow, intermediate marker; green, superficial marker.

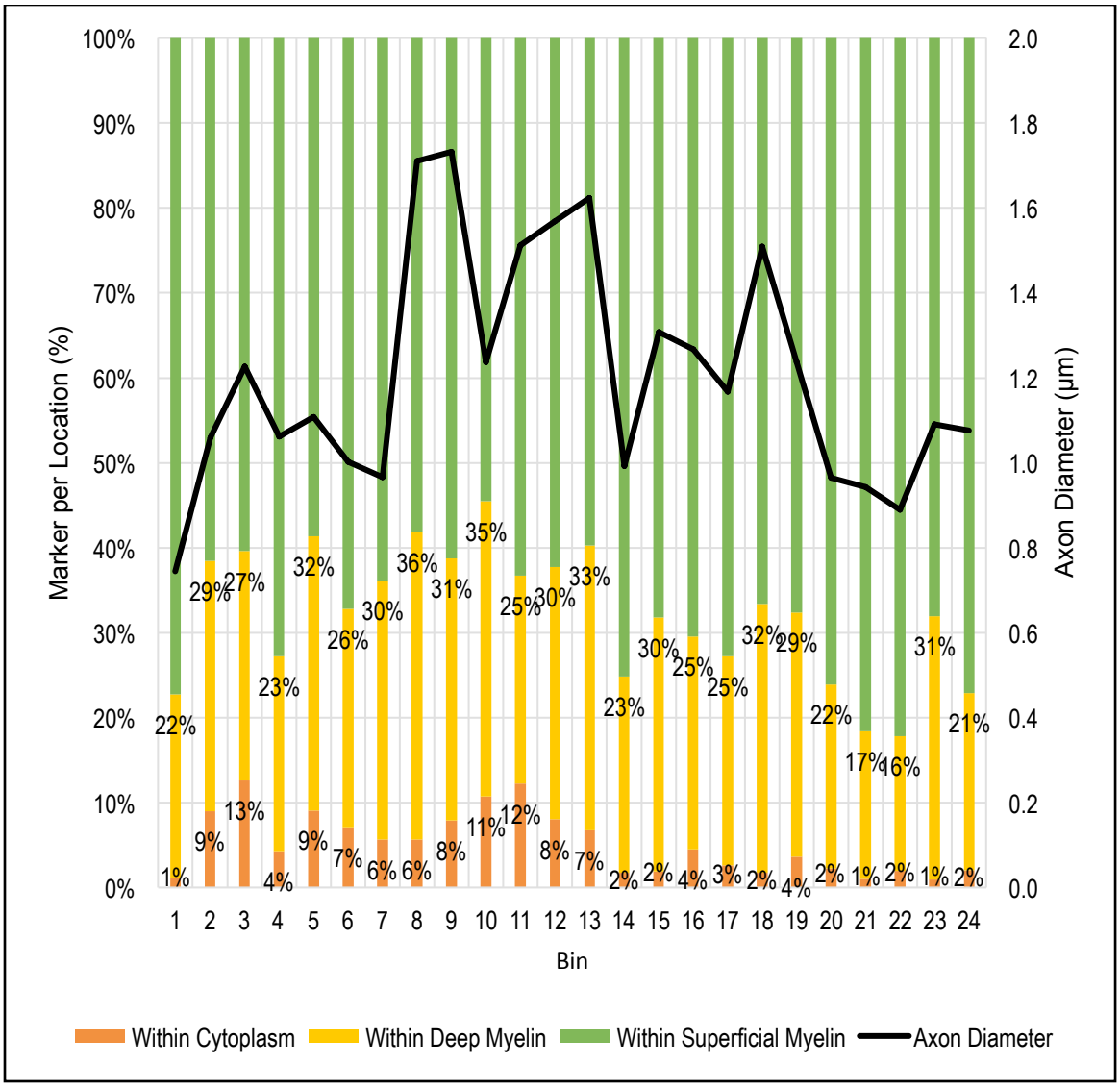

FIGURE 12 Analysis of Axon 4 (Sections = 1–86; Bins = 1–24; length = 26.24 µm). Quantitative analysis of marker category shows proportion relative to site of axon across sections. Each bin represents 1 micron of axon length. Axon diameter represents maximum width within the bin.

In summary, qualitative and quantitative analyses showed that the brevican marker weaves through the membrane of the axon and the myelin sheath. The marker was seen to be consistently found at all depths in varying quantities. These quantities varied in a periodic, wave-like manner along the length of the axon, suggesting a weaving pattern, as seen in the analyses of incidence.

DISCUSSION

The present study provided evidence on the location of PNN and axonal coat elements relative to their associated axons within the MD thalamus. It had been previously thought that PNNs are found exclusively within the surrounding ECM of neurons (Celio et al., 1998; Vitellaro-Zuccarello et al., 1998). My observations and analyses have provided evidence that elements of PNNs form axonal coats that are located within the myelin and the cytoplasm of neurons, in addition to their presence in ECM. Moreover, the present findings reveal that axonal coats have a wave-like formation through the length of axons.

Two-dimensional analyses showed that the brevican marker was more often within the cytoplasm and myelin than solely outside the myelin of axons. The brevican marker was consistently distributed throughout the cytoplasm, myelin, and outside the myelin (within the ECM) of axons. Axon diameter was also greater in axons with the marker within the myelin or cytoplasm. The diameter of axons appeared to increase along with the quantity of PNNs within the myelin and cytoplasm.

Three-dimensional reconstructions showed that axons of greater length within the studied images showed brevican marker both outside and inside the myelin and cytoplasm. These reconstructions showed that axon diameter and quantity of the brevican marker within the myelin and cytoplasm fluctuate consistently along the length of the axon in a periodic, wave-like manner. Together, these data suggest a potential pattern of

PNN elements such that they weave through their associated axons like threads weaving through cloth.

Brevican Found in All Axonal Regions

Observation of brevican in all regions of the axon (cytoplasm, myelin, and outside myelin) provides evidence that PNN elements and axonal coats are found in all these sites. This is supported by a number of studies which focus on the other components of PNNs, specifically hyaluronic acid and tenascin-R (Bruckner et al., 2000; Czopka, Von Holst, Schmidt, Ffrench-Constant, & Faissner, 2009; Gurevicius, Gureviciene, Valjakka, Schachner, & Tanila, 2004; Li, Li, Jin, Wang, & Zhao, 2017; Pesheva, Spiess, & Schachner, 1989; Probstmeier, Stichel, Muller, Asou, & Pesheva, 2000; Ripellino, Klinger, Margolis, & Margolis, 1985).

Hyaluronan provides structure to PNNs, both physically and biochemically (Li et al., 2017). In a study of tau pathology, Li et al. observed that the hyaluronic acid synthase Has1 is found along the length of the axon. This study provided evidence that the regulation of hyaluronan synthase expression and Has1 axonal localization has a direct effect on neuronal plasticity, the key characteristic of PNNs. Co-staining with neuronal markers clearly showed that Has1 was the only hyaluronan synthase located along the axon (Li et al., 2017). The aforementioned study reinforces a previous study which also found evidence of hyaluronan expression along axons of neurons (Ripellino et al., 1985).

Tenascin-R is an ECM protein found in myelin of the CNS. This protein has been associated with inhibiting the outgrowth of neurites (Pesheva, Gennarini, Goridis, & Schachner, 1993; Pesheva et al., 1989). Such inhibition has a clear link to a reduction of plasticity and PNN function. This protein, found along the length of the myelinated membrane of the axon, is associated with an influence on the ionic milieu of the neuron and its immediate surroundings (Probstmeier et al., 2000). Another study showed a similar effect of tenascin-R preventing the formation of myelinated membranes, but more specifically through the use of RhoA pathways (Czopka et al., 2009). Tenascin-R deficient mice have shown a significantly reduced density of PNNs as well as abnormally increased excitatory transmission, suggesting an involvement in the decrease of transmission (Bruckner et al., 2000; Gurevicius et al., 2004).

Several studies thus describe features of axons without directly referencing PNNs or axonal coats (Bruckner et al., 2000; Czopka et al., 2009; Gurevicius et al., 2004; Li et al., 2017; Pesheva et al., 1993; Pesheva et al., 1989; Probstmeier et al., 2000; Ripellino et al., 1985). While these studies focus on distinct structures, they provide indirect information about PNNs since the observed structures are components of PNNs and axonal coats. The common thread of each component, including CSPG, hyaluronan, and tenascin-R, is an impeding influence on plasticity by PNNs.

Axon Diameter and Quantity of Brevican Fluctuate in a Wavelike Manner

The results showed that axon diameter and quantity of brevican fluctuate in a wavelike manner along the length of the neuron. This suggests that PNN elements are located in these regions and weave through the length of the axon with comparable concentrations within the cytoplasm, myelin and ECM. The two-dimensional analysis provided the proportion of PNN elements at three depths, which suggest a possible structure for a weaving pattern. Axons had a distinct proportion of PNN elements in each region of their axons: outside the myelin, within the myelin, and within the cytoplasm. This arrangement was demonstrated by complete reconstruction of a field of axons. The large scale reconstruction showed that the greater the observable length of axons, the greater the likelihood of finding a weaving pattern of marker. This suggests that if PNN elements are seen only on the outside of an axon in a small area, if the area of observation is increased, these elements could eventually be seen to weave through the overall axon. Further evidence for this model, is seen in three-dimensional reconstructions of axons which provided evidence that the axon diameter and quantity of brevican fluctuate periodically within the deep myelin and cytoplasm along the length of the axon. Using these results, Figure 13 shows a model of a potential structure of PNNs.

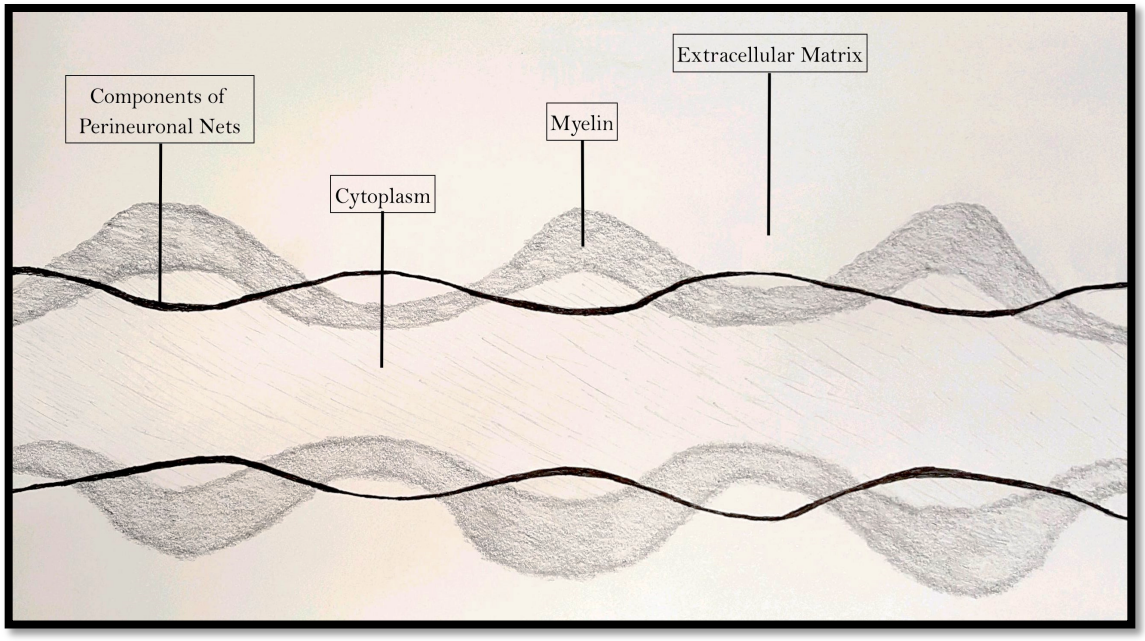

FIGURE 13 Model of marker components of PNNs along an axon. This model reflects the quantitative and qualitative observations.

Functional Implications for a Weaving Structure of Perineuronal Net Elements

PNNs are associated with a decrease in plasticity and an increase of stability of neural systems (Berretta, 2012; Bitanihirwe & Woo, 2014; Bukalo et al., 2001; Carstens et al., 2016; Carulli et al., 2016; Dityatev & Schachner, 2003; Hartig et al., 1999; Karetko & Skangiel-Kramska, 2009; Kauhausen et al., 2015; Kwok et al., 2008; Lendvai et al., 2013; Nabel & Morishita, 2013; Pantazopoulos & Berretta, 2016; D. Wang & Fawcett, 2012). The means by which these structures perform this function is uncertain. The present findings suggest that the location and structure of PNNs relative to the axon play a key role in their influences on plasticity and stability. This is directly linked to two observations from this study: that elements of PNNs and axonal coats are found at all areas/depths of the axon, and that axon diameter and quantity of PNN markers fluctuate

in a periodic manner along the length of the axon. There are a number of functional reasons why elements of PNNs might have this weaving structure as suggested below.

PNNs here were studied through their CSPG brevican element. There are various means by which CSPGs can play a prominent role in the function of PNNs. The neuronal membrane may have designated receptors for CSPGs (Carulli et al., 2005). These receptors could have a number of functions. CSPGs may anchor to growth promoting molecules to prevent access to growth promoting sites (Deepa, Umehara, Higashiyama, Itoh, & Sugahara, 2002; McKeon, Hoke, & Silver, 1995; Smith-Thomas et al., 1995; Snow & Letourneau, 1992). Hindering these molecules would prevent their influence on the overall structural and functional growth of cells, thereby diminishing local plasticity. CSPGs could aid the binding of growth inhibitory molecules (Powell, Fawcett, & Geller, 1997; Smith-Thomas et al., 1995), providing another mechanism to obstruct plasticity by reducing growth and increasing stability of a region. CSPGs might also be a medium by which other molecules can bind to receptors for initiating transmembrane signaling. Through transmembrane signaling CSPGs might heavily influence a number of cellular processes (Borisoff et al., 2003; Monnier, Sierra, Schwab, Henke-Fahle, & Mueller, 2003; Powell, Mercado, Calle-Patino, & Geller, 2001; Sivasankaran et al., 2004).

The unique composition and structure of PNNs could influence ion homeostasis. The presence of PNNs on both sides of the membrane found in this study, suggests an ability to influence ion homeostasis from both sides of ion channels. Ion homeostasis directly influences a neuron's ability to depolarize and transmit an action potential (Barnett & Larkman, 2007). The polyanionic character of PNNs creates a degree of ion

homeostasis within the microenvironment by acting as a buffering system for relevant ions (Bruckner et al., 1993). Such a characteristic prevents the hyperexcitability of neurons, shown in studies focusing on potassium ions (Bitanihirwe & Woo, 2014). Fast-spiking neurons are thought to have a large ionic current across their membranes. This suggests a high influx of sodium ions and high efflux of potassium ions. Such an influx and efflux could be moderated by a buffer system. This system would create local expansions and contractions of extracellular clefts, removing the need for high-magnitude fluxes of ions across short distances (Hartig et al., 1999). The expansions and contractions are consistent with the present structural findings.

There are a number of theories as to how PNNs in general might be involved in ion homeostasis. They might affect the placement or diffusion of ion channels along the plasma membrane. For example, the degradation of PNNs has been associated with an increase in the diffusion of AMPA receptors (Frischknecht et al., 2009). PNNs could also affect the gating subunits of ion channels through their highly anionic character. Such a buffering system would neutralize membrane surface charge and influence channel gating, resulting in a reduction of spiking (Balmer, 2016; Hille, 2001). This arrangement could stabilize the ion microenvironment through buffering. PNN degradation is also associated with an increase in the diffusion of calcium ions, suggesting that the presence of PNNs removes need for the compound effects of these ions. (Balmer, 2016; Hrabetova et al., 2009).

The Role of Perineuronal Nets in Cortico-Thalamo-Cortical Communication

The structure and location of PNNs play a significant role in cortico-thalamo-cortical communication. The influence of PNN elements on plasticity and stability of neural pathways within and through the MD thalamus has far reaching implications, because of its interconnections with the PFC (Barbas et al., 2013; Barbas et al., 1991; Dermon & Barbas, 1994; Giguere & Goldman-Rakic, 1988; Goldman-Rakic & Porrino, 1985; Guillery, 1995; Jones, 1998; McFarland & Haber, 2002; Mitchell, 2015; Ray & Price, 1993; Rose & Woolsey, 1948; Schwartz et al., 1991; Xiao et al., 2009).

The structures of the ECM, including PNNs, are formed and maintained for specific functions of local sites (Alberts, 2002). In a study comparing the concentration of various proteins and structures in regions throughout the brain, PNNs were found in their lowest concentration within the thalamus. Within the thalamus, there were significant differences in the concentrations of PNN related CSPGs between the central nuclei (including the mediodorsal nucleus) and the reticular nucleus, lateral dorsal nucleus, and ventral nuclei (Dauth et al., 2016). These significant differences reflect the unique environment and contents of each of these nuclei. The concentration of PNNs reflects the degree of plasticity and stability of a region (Dauth et al., 2016). The concentration of PNNs within each region and subregion suggests differences in the ability to modify the associated neural pathways.

The PNNs in MD would have a direct impact on its role in cortico-thalamo-cortical communication, particularly the stability and adaptation of associated pathways. The

PFC, the region distinctly associated with the MD thalamus, is highly malleable for exercising a role in executive function (Jung, Baeg, Kim, Kim, & Kim, 2008; Kuboshima-Amemori & Sawaguchi, 2007). The presence and quantity of PNNs within the MD thalamus is distinctly reflective of this relationship (Bueno-Junior, Lopes-Aguiar, Ruggiero, Romcy-Pereira, & Leite, 2012).

In terms of cognitive disorders, schizophrenia is an excellent model to investigate the role of PNNs in this cortico-thalamo-cortical communication, as shown in a recent study of the concentration of PNNs within the PFC focusing on individuals diagnosed with schizophrenia. This study showed that there is a 70–76% decrease of PNNs in layer V of the PFC (Mauney et al., 2013). This is particularly relevant because of the MD thalamus's interconnectivity with this particular layer of the PFC (Mitchell, 2015; Xiao et al., 2009). Since schizophrenia is associated with a decrease in the concentration of PNNs in both the PFC and the MD, this is a clear reflection of the complementary activity and plasticity of these regions.

Conclusions and Future Directions

Using immunohistochemistry and electron microscopy I have observed elements of PNNs to weave through the length of axons in the lateral part of MD thalamus of normal subjects. While animal models, such as rodents and non-human primates, have been used extensively in the past, the work presented here used human tissue. The use of human tissue is needed for future studies to examine both PNNs and the MD thalamus.

While my work has shed light on the nature of PNN elements and axonal coats in the MD thalamic nucleus at the cellular level, future research must expand more specifically on this area. The model that I have described may have a significant influence on neuroplasticity of corticothalamic connections. Future studies may use methods to study this model using a variety of biochemical environments and physiological situations. Such studies could utilize *post-mortem* tissue of individuals diagnosed with cognitive disorders of varying degrees of severity to observe the relative effects on PNN concentration and structure. By observing and analyzing PNNs we may achieve a better understanding of the nature of neuroplasticity at both the cellular and systems levels.

REFERENCES

List of Abbreviated Journal Titles

Acta Neurobiol Exp (Wars.)	Acta Neurobiologiae Experimentalis
Acta Neuropathol	Acta Neuropathologica
Am J Psychiatry	The American Journal of Psychiatry
Ann Neurol	Annals of Neurology
Biol Psychiatry	Biological Psychiatry
Brain Lang	Brain and Language
Brain Res	Brain Research
Br J Psychiatry	The British Journal of Psychiatry
Cell Tissue Res	Cell and Tissue Research
Comput Math Methods Med	Computational and Mathematical Methods in Medicine
Confin Neurol	Confinia Neurologica
Curr Opin Neurobiol	Current Opinion in Neurobiology
Curr Protoc Neurosci	Current Protocols in Neuroscience
Electroenceph Clin Neurophysiol	Electroencephalography and Clinical Neurophysiology
Eur J Neurosci	European Journal of Neuroscience
Eur Psychiatry	European Psychiatry
Exp Neuro	Experimental Neurology
Front Psychiatry	Frontiers in Psychiatry

Front Syst Neurosci	Frontiers in Systems Neuroscience
Ital J Neurol Sci	Italian Journal of Neurological Sciences
J Alzheimers Dis	Journal of Alzheimer's Disease
J Anat	Journal of Anatomy
J Biol Chem	The Journal of Biological Chemistry
J Cell Biol	The Journal of Cell Biology
J Cell Sci	Journal of Cell Science
J Comp Physiol Psychol	Journal of Comparative and Physiological Psychology
J Comp Neurol	Journal of Comparative Neurology
J Neurobiol	Journal of Neurobiology
J Neurochem	Journal of Neurochemistry
J Neurophysiol	Journal of Neurophysiology
J Neurosci	Journal of Neuroscience
J Neurosci Res	Journal of Neuroscience Research
J Physiol	The Journal of Physiology
J Psychiatr Res	Journal of Psychiatric Research
J Psychiatry Neurosci	Journal of Psychiatry & Neuroscience
Mol Cell Neurosci	Molecular and Cellular Neurosciences
Nat Neurosci	Nature Neuroscience
Nat Rev Neurosci	Nature Reviews. Neuroscience
Naunyn Schmiedebergs Arch Exp Pathol Pharmakol	Naunyn-Schmiedebergs Archiv für experimentelle Pathologie und Pharmakologie

Neural Plast	Neural Plasticity
Pract Neurol	Practical Neurology
Restor Neurol Neurosci	Restorative Neurology and Neuroscience
Trends Neurosci	Trends in Neurosciences

References

Aggleton, J. P., & Mishkin, M. (1983a). Memory impairments following restricted medial thalamic lesions in monkeys. *Experimental Brain Research, 52*, 199–209.

Aggleton, J. P., & Mishkin, M. (1983b). Visual recognition impairment following medial thalamic lesions in monkeys. *Neuropsychologia, 21*, 189–197.

Alberts, B. (2002). *Molecular Biology of the Cell* (4 ed.). New York: Garland.

Alelu-Paz, R., & Gimenez-Amaya, J. M. (2008). The mediodorsal thalamic nucleus and schizophrenia. *J Psychiatry Neurosci, 33*(6), 489–498.

Alexander, G. E., & Fuster, J. M. (1973). Effects of cooling prefrontal cortex on cell firing in the nucleus medialis dorsalis. *Brain Research, 61*, 93–105.

Balmer, T. S. (2016). Perineuronal Nets Enhance the Excitability of Fast-Spiking Neurons. *eNeuro, 3*(4). doi: 10.1523/ENEURO.0112-16.2016

Balmer, T. S., Carels, V. M., Frisch, J. L., & Nick, T. A. (2009). Modulation of perineuronal nets and parvalbumin with developmental song learning. *J Neurosci, 29*(41), 12878–12885. doi: 10.1523/JNEUROSCI.2974-09.2009

Barbas, H., García-Cabezas, M. A., & Zikopoulos, B. (2013). Frontal-thalamic circuits associated with language. *Brain Lang, 126*(1), 49–61. doi: 10.1016/j.bandl.2012.10.001

Barbas, H., Henion, T. H., & Dermon, C. R. (1991). Diverse thalamic projections to the prefrontal cortex in the rhesus monkey. *Journal of Comparative Neurology, 313*, 65–94.

Barnett, M. W., & Larkman, P. M. (2007). The action potential. *Pract Neurol, 7*(3), 192–197.

Bear, M. F., Connors, B. W., & Paradiso, M. A. (2007). *Neuroscience: Exploring the Brain*. Philadelphia, PA: Lippincott Williams & Wilkins.

Berendse, H. W., & Groenewegen, H. J. (1990). Organization of the thalamostriatal projections in the rat, with special emphasis on the ventral striatum. *J Comp Neurol, 299*(2), 187–228. doi: 10.1002/cne.902990206

Berretta, S. (2012). Extracellular matrix abnormalities in schizophrenia. *Neuropharmacology, 62*(3), 1584–1597. doi: 10.1016/j.neuropharm.2011.08.010

Bitanihirwe, B. K., & Woo, T. U. (2014). Perineuronal nets and schizophrenia: the importance of neuronal coatings. *Neuroscience and Biobehavioral Reviews, 45*, 85–99. doi: 10.1016/j.neubiorev.2014.03.018

Blosa, M., Sonntag, M., Jager, C., Weigel, S., Seeger, J., Frischknecht, R., . . . Morawski, M. (2015). The extracellular matrix molecule brevican is an integral component of the machinery mediating fast synaptic transmission at the calyx of Held. *J Physiol, 593*(19), 4341–4360. doi: 10.1113/JP270849

Borisoff, J. F., Chan, C. C., Hiebert, G. W., Oschipok, L., Robertson, G. S., Zamboni, R., . . . Tetzlaff, W. (2003). Suppression of Rho-kinase activity promotes axonal growth on inhibitory CNS substrates. *Mol Cell Neurosci, 22*(3), 405–416.

Bradfield, L. A., Hart, G., & Balleine, B. W. (2013). The role of the anterior, mediodorsal, and parafascicular thalamus in instrumental conditioning. *Front Syst Neurosci, 7*, 51. doi: 10.3389/fnsys.2013.00051

Bruckner, G., Brauer, K., Hartig, W., Wolff, J. R., Rickmann, M. J., Derouiche, A., . . . Reichenbach, A. (1993). Perineuronal nets provide a polyanionic, glia-associated form of microenvironment around certain neurons in many parts of the rat brain. *Glia, 8*(3), 183–200. doi: 10.1002/glia.440080306

Bruckner, G., Grosche, J., Schmidt, S., Hartig, W., Margolis, R. U., Delpech, B., . . . Schachner, M. (2000). Postnatal development of perineuronal nets in wild-type mice and in a mutant deficient in tenascin-R. *J Comp Neurol, 428*(4), 616–629.

Bueno-Junior, L. S., Lopes-Aguiar, C., Ruggiero, R. N., Romcy-Pereira, R. N., & Leite, J. P. (2012). Muscarinic and nicotinic modulation of thalamo-prefrontal cortex synaptic plasticity [corrected] in vivo. *PLoS One, 7*(10), e47484. doi: 10.1371/journal.pone.0047484

Bukalo, O., Schachner, M., & Dityatev, A. (2001). Modification of extracellular matrix by enzymatic removal of chondroitin sulfate and by lack of tenascin-R differentially affects several forms of synaptic plasticity in the hippocampus. *Neuroscience, 104*(2), 359–369.

Byne, W., Buchsbaum, M. S., Mattiace, L. A., Hazlett, E. A., Kemether, E., Elhakem, S. L., . . . Jones, L. (2002). Postmortem assessment of thalamic nuclear volumes in subjects with schizophrenia. *Am J Psychiatry, 159*(1), 59–65. doi: 10.1176/appi.ajp.159.1.59

Carlesimo, G. A., Costa, A., Serra, L., Bozzali, M., Fadda, L., & Caltagirone, C. (2011). Prospective memory in thalamic amnesia. *Neuropsychologia, 49*(8), 2199–2208. doi: 10.1016/j.neuropsychologia.2010.11.013

Carstens, K. E., Phillips, M. L., Pozzo-Miller, L., Weinberg, R. J., & Dudek, S. M. (2016). Perineuronal Nets Suppress Plasticity of Excitatory Synapses on CA2 Pyramidal Neurons. *J Neurosci, 36*(23), 6312–6320. doi: 10.1523/JNEUROSCI.0245-16.2016

Carulli, D., Kwok, J. C., & Pizzorusso, T. (2016). Perineuronal Nets and CNS Plasticity and Repair. *Neural Plast, 2016*, 4327082. doi: 10.1155/2016/4327082

Carulli, D., Laabs, T., Geller, H. M., & Fawcett, J. W. (2005). Chondroitin sulfate proteoglycans in neural development and regeneration. *Curr Opin Neurobiol, 15*(1), 116–120. doi: 10.1016/j.conb.2005.01.014

Carulli, D., Pizzorusso, T., Kwok, J. C., Putignano, E., Poli, A., Forostyak, S., . . . Fawcett, J. W. (2010). Animals lacking link protein have attenuated perineuronal nets and persistent plasticity. *Brain, 133*(Pt 8), 2331–2347. doi: 10.1093/brain/awq145

Carulli, D., Rhodes, K. E., & Fawcett, J. W. (2007). Upregulation of aggrecan, link protein 1, and hyaluronan synthases during formation of perineuronal nets in the rat cerebellum. *J Comp Neurol, 501*(1), 83–94. doi: 10.1002/cne.21231

Celio, M. R., Spreafico, R., De Biasi, S., & Vitellaro-Zuccarello, L. (1998). Perineuronal nets: past and present. *Trends Neurosci, 21*(12), 510–515.

Crair, M. C., & Malenka, R. C. (1995). A critical period for long-term potentiation at thalamocortical synapses. *Nature, 375*(6529), 325–328. doi: 10.1038/375325a0

Czopka, T., Von Holst, A., Schmidt, G., Ffrench-Constant, C., & Faissner, A. (2009). Tenascin C and tenascin R similarly prevent the formation of myelin membranes in a RhoA-dependent manner, but antagonistically regulate the expression of myelin basic protein via a separate pathway. *Glia, 57*(16), 1790–1801. doi: 10.1002/glia.20891

Dauth, S., Grevesse, T., Pantazopoulos, H., Campbell, P. H., Maoz, B. M., Berretta, S., & Parker, K. K. (2016). Extracellular matrix protein expression is brain region dependent. *J Comp Neurol, 524*(7), 1309–1336. doi: 10.1002/cne.23965

Deepa, S. S., Umehara, Y., Higashiyama, S., Itoh, N., & Sugahara, K. (2002). Specific molecular interactions of oversulfated chondroitin sulfate E with various heparin-binding growth factors. Implications as a physiological binding partner in the brain and other tissues. *J Biol Chem, 277*(46), 43707–43716. doi: 10.1074/jbc.M207105200

Dermon, C. R., & Barbas, H. (1994). Contralateral thalamic projections predominantly reach transitional cortices in the rhesus monkey. *J Comp Neurol, 344*, 508–531.

Dhir, A. (2012). Pentylenetetrazol (PTZ) kindling model of epilepsy. *Curr Protoc Neurosci, Chapter 9*, Unit9.37. doi: 10.1002/0471142301.ns0937s58

Dityatev, A., & Schachner, M. (2003). Extracellular matrix molecules and synaptic plasticity. *Nat Rev Neurosci, 4*(6), 456–468. doi: 10.1038/nrn1115

Edelstyn, N. M., Grange, J. A., Ellis, S. J., & Mayes, A. R. (2016). A deficit in familiarity-driven recognition in a right-sided mediodorsal thalamic lesion patient. *Neuropsychology, 30*(2), 213–224. doi: 10.1037/neu0000226

Fiala, J. C. (2005). Reconstruct: a free editor for serial section microscopy. *Journal of Microscopy, 218*(Pt 1), 52–61.

Frischknecht, R., Heine, M., Perrais, D., Seidenbecher, C. I., Choquet, D., & Gundelfinger, E. D. (2009). Brain extracellular matrix affects AMPA receptor lateral mobility and short-term synaptic plasticity. *Nat Neurosci, 12*(7), 897–904. doi: 10.1038/nn.2338

Friston, K. J., & Frith, C. D. (1995). Schizophrenia: a disconnection syndrome? *Clinical Neuroscience, 3*, 89–97.

Fuster, J. M. (2008). *The prefrontal cortex* (4th ed.). London (UK): Elsevier/Academic Press.

Fuster, J. M., & Alexander, G. E. (1973). Firing changes in cells of the nucleus medialis dorsalis associated with delayed response behavior. *Brain Research, 61*, 79–91.

Gaffan, D. (2002). Amnesia for complex naturalistic scenes and for objects following fornix transection in the rhesus monkey. *Eur. J Neurosci., 4*, 381–388.

Gaffan, D., & Murray, E. A. (1990). Amygdalar interaction with the mediodorsal nucleus of the thalamus and the ventromedial prefrontal cortex in stimulus reward associative learning in the monkey. *Journal of Neuroscience, 10*, 3479–3493.

Gaffan, D., & Parker, A. (2000). Mediodorsal thalamic function in scene memory in rhesus monkeys. *Brain, 123*, 816–827.

Gaffan, D., & Watkins, S. (1991). Mediodorsal Thalamic Lesions Impair Long-Term Visual Associative Memory in Macaques. *Eur J Neurosci, 3*(7), 615–620.

Giguere, M., & Goldman-Rakic, P. S. (1988). Mediodorsal nucleus: Areal, laminar, and tangential distribution of afferents and efferents in the frontal lobe of rhesus monkeys. *J Comp Neurol, 277*, 195–213.

Gimenez-Amaya, J. M., McFarland, N. R., de las Heras, S., & Haber, S. N. (1995). Organization of thalamic projections to the ventral striatum in the primate. *Journal of Comparative Neurology, 354*, 127–149.

Gogolla, N., Caroni, P., Luthi, A., & Herry, C. (2009). Perineuronal nets protect fear memories from erasure. *Science, 325*(5945), 1258–1261. doi: 10.1126/science.1174146

Goldman-Rakic, P. S., & Porrino, L. J. (1985). The primate mediodorsal (MD) nucleus and its projection to the frontal lobe. *Journal of Comparative Neurology, 242*, 535–560.

Groenewegen, H. J., Berendse, H. W., Wolters, J. G., & Lohman, A. H. (1990). The anatomical relationship of the prefrontal cortex with the striatopallidal system, the thalamus and the amygdala: evidence for a parallel organization. *Progress in Brain Research, 85*, 95–116.

Groenewegen, H. J., Galis-de Graaf, Y., & Smeets, W. J. (1999). Integration and segregation of limbic cortico-striatal loops at the thalamic level: an experimental tracing study in rats. *Journal of Chemical Neuroanatomy, 16*, 167–185.

Guillery, R. W. (1995). Anatomical evidence concerning the role of the thalamus in corticocortical communication: a brief review. *J Anat., 187 (Pt 3)*, 583–592.

Gurevicius, K., Gureviciene, I., Valjakka, A., Schachner, M., & Tanila, H. (2004). Enhanced cortical and hippocampal neuronal excitability in mice deficient in the extracellular matrix glycoprotein tenascin-R. *Mol Cell Neurosci, 25*(3), 515–523. doi: 10.1016/j.mcn.2003.12.001

Haber, S. N., & Calzavara, R. (2009). The cortico-basal ganglia integrative network: the role of the thalamus. *Brain Research Bulletin, 78*(2–3), 69–74. doi: 10.1016/j.brainresbull.2008.09.013

Haber, S. N., & McFarland, N. R. (2001). The place of the thalamus in frontal cortical-basal ganglia circuits. *Neuroscientist., 7*(4), 315–324.

Hartig, W., Derouiche, A., Welt, K., Brauer, K., Grosche, J., Mader, M., . . . Bruckner, G. (1999). Cortical neurons immunoreactive for the potassium channel Kv3.1b subunit are predominantly surrounded by perineuronal nets presumed as a buffering system for cations. *Brain Res, 842*(1), 15–29.

Herry, C., Vouimba, R. M., & Garcia, R. (1999). Plasticity in the mediodorsal thalamo-prefrontal cortical transmission in behaving mice. *J Neurophysiol, 82*(5), 2827–2832.

Hille, B. (2001). *Ion Channels of Excitable Membranes* (3 ed.). Sunderland, MA: Sinauer Associates.

Hrabetova, S., Masri, D., Tao, L., Xiao, F., & Nicholson, C. (2009). Calcium diffusion enhanced after cleavage of negatively charged components of brain extracellular matrix by chondroitinase ABC. *J Physiol, 587*(Pt 16), 4029–4049. doi: 10.1113/jphysiol.2009.170092

Hubel, D. H., & Wiesel, T. N. (1964). Effects of Monocular Deprivation in Kittens. *Naunyn Schmiedebergs Arch Exp Pathol Pharmakol, 248*, 492–497.

Isseroff, A., Rosvold, H. E., Galkin, T. W., & Goldman-Rakic, P. S. (1982). Spatial memory impairments following damage to the mediodorsal nucleus of the thalamus in rhesus monkeys. *Brain Research, 232*, 97–113.

Janssen, J., Aleman-Gomez, Y., Reig, S., Schnack, H. G., Parellada, M., Graell, M., . . . Desco, M. (2012). Regional specificity of thalamic volume deficits in male adolescents with early-onset psychosis. *Br J Psychiatry, 200*(1), 30–36. doi: 10.1192/bjp.bp.111.093732

Jones, E. G. (1998). Viewpoint: the core and matrix of thalamic organization. *Neuroscience, 85*, 331–345.

Jones, E. G. (2007). *The Thalamus*. New York: Cambridge University Press.

Jung, M. W., Baeg, E. H., Kim, M. J., Kim, Y. B., & Kim, J. J. (2008). Plasticity and memory in the prefrontal cortex. *Reviews in the Neurosciences, 19*(1), 29–46.

Karetko, M., & Skangiel-Kramska, J. (2009). Diverse functions of perineuronal nets. *Acta Neurobiol Exp (Wars), 69*(4), 564–577.

Kauhausen, J. A., Thompson, L. H., & Parish, C. L. (2015). Chondroitinase improves midbrain pathway reconstruction by transplanted dopamine progenitors in Parkinsonian mice. *Mol Cell Neurosci, 69*, 22–29. doi: 10.1016/j.mcn.2015.10.002

Kim, D. J., Kim, J. J., Park, J. Y., Lee, S. Y., Kim, J., Kim, I. Y., . . . Park, H. J. (2008). Quantification of thalamocortical tracts in schizophrenia on probabilistic maps. *NeuroReport, 19*(4), 399–403. doi: 10.1097/WNR.0b013e3282f56634

Kito, S., Jung, J., Kobayashi, T., & Koga, Y. (2009). Fiber tracking of white matter integrity connecting the mediodorsal nucleus of the thalamus and the prefrontal cortex in schizophrenia: a diffusion tensor imaging study. *Eur Psychiatry, 24*(5), 269–274. doi: 10.1016/j.eurpsy.2008.12.012

Kuboshima-Amemori, S., & Sawaguchi, T. (2007). Plasticity of the primate prefrontal cortex. *Neuroscientist, 13*(3), 229–240. doi: 10.1177/1073858406298554

Kucharova, K., & Stallcup, W. B. (2010). The NG2 proteoglycan promotes oligodendrocyte progenitor proliferation and developmental myelination. *Neuroscience, 166*(1), 185–194. doi: 10.1016/j.neuroscience.2009.12.014

Kwok, J. C., Afshari, F., Garcia-Alias, G., & Fawcett, J. W. (2008). Proteoglycans in the central nervous system: plasticity, regeneration and their stimulation with chondroitinase ABC. *Restor Neurol Neurosci, 26*(2–3), 131–145.

Lau, L. W., Keough, M. B., Haylock-Jacobs, S., Cua, R., Doring, A., Sloka, S., . . . Yong, V. W. (2012). Chondroitin sulfate proteoglycans in demyelinated lesions impair remyelination. *Ann Neurol, 72*(3), 419–432. doi: 10.1002/ana.23599

LeBlanc, J. J., & Fagiolini, M. (2011). Autism: a "critical period" disorder? *Neural Plast, 2011*, 921680. doi: 10.1155/2011/921680

Lendvai, D., Morawski, M., Negyessy, L., Gati, G., Jager, C., Baksa, G., . . . Alpar, A. (2013). Neurochemical mapping of the human hippocampus reveals perisynaptic matrix around functional synapses in Alzheimer's disease. *Acta Neuropathol, 125*(2), 215–229. doi: 10.1007/s00401-012-1042-0

Li, Y., Li, Z. X., Jin, T., Wang, Z. Y., & Zhao, P. (2017). Tau Pathology Promotes the Reorganization of the Extracellular Matrix and Inhibits the Formation of Perineuronal Nets by Regulating the Expression and the Distribution of Hyaluronic Acid Synthases. *J Alzheimers Dis, 57*(2), 395–409. doi: 10.3233/JAD-160804

Martins-de-Souza, D., Maccarrone, G., Wobrock, T., Zerr, I., Gormanns, P., Reckow, S., . . . Turck, C. W. (2010). Proteome analysis of the thalamus and cerebrospinal fluid reveals glycolysis dysfunction and potential biomarkers candidates for schizophrenia. *J Psychiatr Res, 44*(16), 1176–1189. doi: 10.1016/j.jpsychires.2010.04.014

Mauney, S. A., Athanas, K. M., Pantazopoulos, H., Shaskan, N., Passeri, E., Berretta, S., & Woo, T. U. (2013). Developmental pattern of perineuronal nets in the human prefrontal cortex and their deficit in schizophrenia. *Biol Psychiatry, 74*(6), 427–435. doi: 10.1016/j.biopsych.2013.05.007

McFarland, N. R., & Haber, S. N. (2002). Thalamic relay nuclei of the basal ganglia form both reciprocal and nonreciprocal cortical connections, linking multiple frontal cortical areas. *J Neurosci, 22*(18), 8117–8132.

McKeon, R. J., Hoke, A., & Silver, J. (1995). Injury-induced proteoglycans inhibit the potential for laminin-mediated axon growth on astrocytic scars. *Exp Neurol, 136*(1), 32–43. doi: 10.1006/exnr.1995.1081

Mendonca, P. R., Vargas-Caballero, M., Erdelyi, F., Szabo, G., Paulsen, O., & Robinson, H. P. (2016). Stochastic and deterministic dynamics of intrinsically irregular firing in cortical inhibitory interneurons. *Elife, 5*. doi: 10.7554/eLife.16475

Mitchell, A. S. (2015). The mediodorsal thalamus as a higher order thalamic relay nucleus important for learning and decision-making. *Neuroscience and Biobehavioral Reviews, 54*, 76–88. doi: 10.1016/j.neubiorev.2015.03.001

Mitchell, A. S., Browning, P. G., & Baxter, M. G. (2007). Neurotoxic lesions of the medial mediodorsal nucleus of the thalamus disrupt reinforcer devaluation effects in rhesus monkeys. *Journal of Neuroscience, 27*(42), 11289–11295.

Mitchell, A. S., & Chakraborty, S. (2013). What does the mediodorsal thalamus do? *Front Syst Neurosci, 7*, 37. doi: 10.3389/fnsys.2013.00037

Mitchell, A. S., & Gaffan, D. (2008). The magnocellular mediodorsal thalamus is necessary for memory acquisition, but not retrieval. *J Neurosci, 28*(1), 258–263. doi: 10.1523/JNEUROSCI.4922-07.2008

Monnier, P. P., Sierra, A., Schwab, J. M., Henke-Fahle, S., & Mueller, B. K. (2003). The Rho/ROCK pathway mediates neurite growth-inhibitory activity associated with the chondroitin sulfate proteoglycans of the CNS glial scar. *Mol Cell Neurosci, 22*(3), 319–330.

Nabel, E. M., & Morishita, H. (2013). Regulating critical period plasticity: insight from the visual system to fear circuitry for therapeutic interventions. *Front Psychiatry, 4*, 146. 110.3389/fpsyt.2013.00146. doi: 10.3389/fpsyt.2013.00146

Nathan, M. A., & Smith, O. A., Jr. (1971). Conditional cardiac and suppression responses after lesions in the dorsomedial thalamus of monkeys. *J Comp Physiol Psychol, 76*(1), 66–73.

Ouhaz, Z., Ba-M'hamed, S., & Bennis, M. (2017). Morphological, structural, and functional alterations of the prefrontal cortex and the basolateral amygdala after early lesion of the rat mediodorsal thalamus. *Brain Structure & Function, 222*(6), 2527–2545. doi: 10.1007/s00429-016-1354-2

Pakkenberg, B. (1990). Pronounced reduction of total neuron number in mediodorsal thalamic nucleus and nucleus accumbens in schizophrenics. *Archives of General Psychiatry, 47*, 1023–1028.

Pantazopoulos, H., & Berretta, S. (2016). In Sickness and in Health: Perineuronal Nets and Synaptic Plasticity in Psychiatric Disorders. *Neural Plast, 2016*, 9847696. doi: 10.1155/2016/9847696

Pantazopoulos, H., Woo, T. U., Lim, M. P., Lange, N., & Berretta, S. (2010). Extracellular matrix-glial abnormalities in the amygdala and entorhinal cortex of subjects diagnosed with schizophrenia. *Archives of General Psychiatry, 67*(2), 155–166. doi: 10.1001/archgenpsychiatry.2009.196

Parker, A., Eacott, M. J., & Gaffan, D. (1997). The recognition memory deficit caused by mediodorsal thalamic lesion in non-human primates: a comparison with rhinal cortex lesion. *European Journal of Neuroscience, 9*, 2423–2431.

Parnaudeau, S., O'Neill, P. K., Bolkan, S. S., Ward, R. D., Abbas, A. I., Roth, B. L., . . . Kellendonk, C. (2013). Inhibition of mediodorsal thalamus disrupts thalamofrontal connectivity and cognition. *Neuron, 77*(6), 1151–1162. doi: 10.1016/j.neuron.2013.01.038

Pendleton, J. C., Shamblott, M. J., Gary, D. S., Belegu, V., Hurtado, A., Malone, M. L., & McDonald, J. W. (2013). Chondroitin sulfate proteoglycans inhibit oligodendrocyte myelination through PTPsigma. *Exp Neurol, 247*, 113–121. doi: 10.1016/j.expneurol.2013.04.003

Penfield, W. (1954). Clinical observations on epileptic mechanisms. In W. Penfield & H. Jasper (Eds.), *Epilepsy and the functional anatomy of the human brain*. Boston: Little, Brown and Company.

Pesheva, P., Gennarini, G., Goridis, C., & Schachner, M. (1993). The F3/11 cell adhesion molecule mediates the repulsion of neurons by the extracellular matrix glycoprotein J1-160/180. *Neuron, 10*(1), 69–82.

Pesheva, P., Spiess, E., & Schachner, M. (1989). J1-160 and J1-180 are oligodendrocyte-secreted nonpermissive substrates for cell adhesion. *J Cell Biol, 109*(4 Pt 1), 1765–1778.

Peters, A., Palay, S. L., & Webster, H. D. (1991). *The fine structure of the nervous system. Neurons and their supporting cells* (3rd ed. Vol. 3). New York: Oxford University Press.

Pizzorusso, T., Medini, P., Berardi, N., Chierzi, S., Fawcett, J. W., & Maffei, L. (2002). Reactivation of ocular dominance plasticity in the adult visual cortex. *Science, 298*(5596), 1248–1251. doi: 10.1126/science.1072699

Popken, G. J., Bunney, W. E., Jr., Potkin, S. G., & Jones, E. G. (2000). Subnucleus-specific loss of neurons in medial thalamus of schizophrenics. *Proceedings of the National Academy of Sciences of the United States of America, 97*, 9276–9280.

Powell, E. M., Fawcett, J. W., & Geller, H. M. (1997). Proteoglycans provide neurite guidance at an astrocyte boundary. *Mol Cell Neurosci, 10*(1–2), 27–42. doi: 10.1006/mcne.1997.0629

Powell, E. M., Mercado, M. L., Calle-Patino, Y., & Geller, H. M. (2001). Protein kinase C mediates neurite guidance at an astrocyte boundary. *Glia, 33*(4), 288–297.

Probstmeier, R., Stichel, C. C., Muller, H. W., Asou, H., & Pesheva, P. (2000). Chondroitin sulfates expressed on oligodendrocyte-derived tenascin-R are involved in neural cell recognition. Functional implications during CNS development and regeneration. *J Neurosci Res, 60*(1), 21–36. doi: 10.1002/(SICI)1097-4547(20000401)60:1<21::AID-JNR3>3.0.CO;2-H

Racine, R. J. (1972). Modification of seizure activity by electrical stimulation: II. Motor seizure. *Electroenceph Clin Neurophysiol, 32*, 281–294.

Rankin-Gee, E. K., McRae, P. A., Baranov, E., Rogers, S., Wandrey, L., & Porter, B. E. (2015). Perineuronal net degradation in epilepsy. *Epilepsia, 56*(7), 1124–1133. doi: 10.1111/epi.13026

Ray, J. P., & Price, J. L. (1993). The organization of projections from the mediodorsal nucleus of the thalamus to orbital and medial prefrontal cortex in macaque monkeys. *Journal of Comparative Neurology, 337*, 1–31.

Ripellino, J. A., Klinger, M. M., Margolis, R. U., & Margolis, R. K. (1985). The hyaluronic acid binding region as a specific probe for the localization of hyaluronic acid in tissue sections. Application to chick embryo and rat brain. *Journal of Histochemistry and Cytochemistry, 33*(10), 1060–1066. doi: 10.1177/33.10.4045184

Romberg, C., Yang, S., Melani, R., Andrews, M. R., Horner, A. E., Spillantini, M. G., . . . Saksida, L. M. (2013). Depletion of perineuronal nets enhances recognition memory and long-term depression in the perirhinal cortex. *J Neurosci, 33*(16), 7057–7065. doi: 10.1523/JNEUROSCI.6267-11.2013

Rose, J. E., & Woolsey, C. N. (1948). The orbitofrontal cortex and its connections with the mediodorsal nucleus in rabbit, sheep and cat. *Research Publications-Association for Research in Nervous and Mental Disease, 27*, 210–232.

Schwartz, M. L., Dekker, J. J., & Goldman-Rakic, P. S. (1991). Dual mode of corticothalamic synaptic termination in the mediodorsal nucleus of the rhesus monkey. *Journal of Comparative Neurology, 309*, 289–304.

Sherman, S. M., & Guillery, R. W. (2006). *Exploring the Thalamus and Its Role in Cortical Function*. Cambridge, MA: MIT Press.

Sherman, S. M., & Guillery, R. W. (2013). *Functional Connections of Cortical Areas: A New View from the Thalamus*. Cambridge, MA: MIT Press.

Siebert, J. R., & Osterhout, D. J. (2011). The inhibitory effects of chondroitin sulfate proteoglycans on oligodendrocytes. *J Neurochem, 119*(1), 176–188. doi: 10.1111/j.1471-4159.2011.07370.x

Sivasankaran, R., Pei, J., Wang, K. C., Zhang, Y. P., Shields, C. B., Xu, X. M., & He, Z. (2004). PKC mediates inhibitory effects of myelin and chondroitin sulfate proteoglycans on axonal regeneration. *Nat Neurosci, 7*(3), 261–268. doi: 10.1038/nn1193

Smith-Thomas, L. C., Stevens, J., Fok-Seang, J., Faissner, A., Rogers, J. H., & Fawcett, J. W. (1995). Increased axon regeneration in astrocytes grown in the presence of proteoglycan synthesis inhibitors. *J Cell Sci, 108 (Pt 3)*, 1307–1315.

Snow, D. M., & Letourneau, P. C. (1992). Neurite outgrowth on a step gradient of chondroitin sulfate proteoglycan (CS-PG). *J Neurobiol, 23*(3), 322–336. doi: 10.1002/neu.480230311

Spiegel, E. A., & Wycis, H. T. (1967). Multiple representation of various functions in the human subcortex. *Confin Neurol, 29*(2), 163–167.

Timbie, C., & Barbas, H. (2014). Specialized pathways from the primate amygdala to posterior orbitofrontal cortex. *J Neurosci, 34*(24), 8106–8118.

Timbie, C., & Barbas, H. (2015). Pathways for emotions: Specializations in the amygdalar, mediodorsal thalamic, and posterior orbitofrontal network. *J Neurosci, 35*(34), 11976–11987.

Tovote, P., Esposito, M. S., Botta, P., Chaudun, F., Fadok, J. P., Markovic, M., . . . Luthi, A. (2016). Midbrain circuits for defensive behaviour. *Nature, 534*(7606), 206–212. doi: 10.1038/nature17996

Van der Werf, Y. D., Scheltens, P., Lindeboom, J., Witter, M. P., Uylings, H. B., & Jolles, J. (2003). Deficits of memory, executive functioning and attention following infarction in the thalamus; a study of 22 cases with localised lesions. *Neuropsychologia, 41*(10), 1330–1344.

Van der Werf, Y. D., Witter, M. P., Uylings, H. B., & Jolles, J. (2000). Neuropsychology of infarctions in the thalamus: a review. *Neuropsychologia, 38*(5), 613–627.

Vitellaro-Zuccarello, L., De Biasi, S., & Spreafico, R. (1998). One hundred years of Golgi's "perineuronal net": history of a denied structure. *Ital J Neurol Sci, 19*(4), 249–253.

Wang, D., & Fawcett, J. (2012). The perineuronal net and the control of CNS plasticity. *Cell Tissue Res, 349*(1), 147–160. doi: 10.1007/s00441-012-1375-y

Wang, T. Y., Bruggeman, K. F., Kauhausen, J. A., Rodriguez, A. L., Nisbet, D. R., & Parish, C. L. (2016). Functionalized composite scaffolds improve the engraftment of transplanted dopaminergic progenitors in a mouse model of Parkinson's disease. *Biomaterials, 74*, 89–98. doi: 10.1016/j.biomaterials.2015.09.039

Watanabe, Y., & Funahashi, S. (2012). Thalamic mediodorsal nucleus and working memory. *Neuroscience and Biobehavioral Reviews, 36*(1), 134–142. doi: 10.1016/j.neubiorev.2011.05.003

Williams, D. (1953). A study of thalamic and cortical rhythms in petit mal. *Brain, 76*(1), 50–69.

Wilson, C. R., & Gaffan, D. (2008). Prefrontal-inferotemporal interaction is not always necessary for reversal learning. *J Neurosci, 28*(21), 5529–5538. doi: 10.1523/JNEUROSCI.0952-08.2008

Xiao, D., Zikopoulos, B., & Barbas, H. (2009). Laminar and modular organization of prefrontal projections to multiple thalamic nuclei. *Neuroscience, 161*(4), 1067–1081.

Yamada, J., & Jinno, S. (2017). Molecular heterogeneity of aggrecan-based perineuronal nets around five subclasses of parvalbumin-expressing neurons in the mouse hippocampus. *J Comp Neurol, 525*(5), 1234–1249. doi: 10.1002/cne.24132

Zhang, Z., Li, J. J., Lu, Q. C., Gong, H. Q., Liang, P. J., & Zhang, P. M. (2016). Interaction between Thalamus and Hippocampus in Termination of Amygdala-Kindled Seizures in Mice. *Comput Math Methods Med, 2016*, 9580724. doi: 10.1155/2016/9580724

Zikopoulos, B., & Barbas, H. (2006). Prefrontal projections to the thalamic reticular nucleus form a unique circuit for attentional mechanisms. *Journal of Neuroscience, 26*, 7348–7361.

Zikopoulos, B., & Barbas, H. (2007). Parallel driving and modulatory pathways link the prefrontal cortex and thalamus *PLoS One, 2*(9), e848. doi: 10.1371/journal.pone.0000848

Zikopoulos, B., & Barbas, H. (2010). Changes in prefrontal axons may disrupt the network in autism. *Journal of Neuroscience, 30*(44), 14595–14609.

Zola-Morgan, S., & Squire, L. R. (1985). Amnesia in monkeys after lesions of the mediodorsal nucleus of the thalamus. *Annals of Neurology, 17*, 558–564.

CURRICULUM VITAE